Advanced Industrial and Engineering Polymer Research 7 (2024) 405–427

Contents lists available at ScienceDirect

Advanced Industrial and Engineering Polymer Research

journal homepage: http://www.keaipublishing.com/aiepr

Effect of nanofillers addition on the compatibilization of polymer blends

Andrea Dorigato*, Giulia Fredi

University of Trento, Department of Industrial Engineering, Via Sommarive 9 38123 Trento, Italy

ARTICLE INFO

Article history:
Received 6 April 2023
Received in revised form
8 August 2023
Accepted 18 September 2023

Keywords:
Blends
Compatibilization
Nanofiller
Microstructure
Physical properties

ABSTRACT

The recent interest in multifunctional materials with tailorable performances led to the formulation of novel polymer blends, with enhanced properties with respect to traditional plastics and showing economical advantages compared to the synthesis of new polymers. However, polymer blends are immiscible in most cases, and proper compatibilization is therefore needed to obtain an alloy with suitable performances. Beside the traditional compatibilization approaches (i.e., addition of graft or branched copolymers, reactive compatibilization), a novel technique has recently emerged, based on the insertion of micro- and nanostructured inorganic fillers within polymer blends.

Therefore, the aim of this review is to give an overview about the role played by nanofillers on the compatibilization of polymer alloys. A survey of the most important papers in literature on this topic will be presented, trying to correlate the microstructural features of nanofilled blends to their physical properties. After an introduction on the general aspects of polymer alloys in Chapter 1, the most relevant compatibilization strategies will be presented in Chapter 2, with particular emphasis on the compatibilization induced by micro- and nanostructured fillers. Chapter 3 will be focused on the nanofiller induced compatibilization, and several examples of thermoplastic, thermosetting and elastomeric nanofilled blends will be presented. Considering the increasing importance of biopolymers and of their blends in the modern industry, in Chapter 4 it will be shown how nanofiller induced compatibilization could be successfully applied also to bioplastics based alloys. Due to the recent environmental concerns on the polymer waste management and the difficulties in the plastics sorting operations, in Chapter 5 it will be demonstrated that nanomodification of recycled plastics can lead to blend recyclates with good compatibility and suitable physical properties. The key aspects of the nanofiller induced compatibilization in polymer blends and the future perspectives will be summarized in Chapter 6.

1. General features of polymer blends

The world production of plastics in 1900 was about 30,000 tons, while the global polymer production reached 350 MT in 2017, and 368 MT in 2019, with a saturation level expected to be reached in the middle of the 21st century [1]. Polymers are nowadays the fastest growing materials, and already in 1992 the annual global production of plastics more than doubled in volume that of steel, and nearly tripled its value. It is also important to underline that polymer blends sector within the plastic industry is increasing at a rate about three times higher than the whole [2].

According to the definition provided in literature, a polymer blend can be considered as a mixture of at least two macromolecular substances, polymers or copolymers, at a relative concentration higher than 2 wt% [3]. The continuously increasing interest on polymer alloys is related to the possibility of developing novel polymers with tailor made properties, different from those of the components, solving thus the technical problems due to the synthesis of novel matrices, with considerable economical advantages [4–6]. In other words, polymer blends technology can provide materials with a full set of desired (or improved) properties at limited price, also offering an innovative approach for an efficient industrial and/or municipal plastics waste recycling. The interest of the plastics manufacturers on these materials is related to the possibility to achieve improved processability and elevated versatility, with a reduction of the number of grades that need to

* Corresponding author.
E-mail address: andrea.dorigato@unitn.it (A. Dorigato).

https://doi.org/10.1016/j.aiepr.2023.09.004

List of acronyms

PARA	Amorphous polyamide
AR	Aspect ratio
BT	Barium titanate
bioPE	Bio-polyethylene
bioPET	Bio-poly(ethylene terephthalate)
CB	Carbon black
CNTs	Carbon nanotubes
CO	Cardanol oil
CR	Chloroprene rubber
CA	Citric acid
DSC	Differential scanning calorimetry
ECH	Epichlorohydrin
SBSe	Epoxidized styrene-butadiene-styrene rubber
EAMAT	Ethylene-acrylic ester-maleic anhydride terpolymer
EGMA	Ethylene/methylacrylate/glycidyl methacrylate copolymer
EPC	Ethylene-propylene copolymer
EPDM	Ethylene propylene diene monomers
EPR	Ethylene propylene rubber
FT-IR	Fourier-transform infrared spectroscopy
PS-g-PA6	Graft copolymer of PS and PA6
GO	Graphene oxide
GnP	Graphite nanoplatelets
HDT	Heat deflection temperature
HDPE	High density polyethylene
HIPS	High impact polystyrene
SEP	Hydrogenated butadiene-b-isoprene-b-styrene
SEB	Hydrogenated butadiene-b-styrene
SEBS	Hydrogenated styrene-butadiene-styrene triblock copolymer
LS	Light scattering
LDPE	Low density polyethylene
LCST	Lower critical solution temperature
ABS-MA	Maleic anhydride-grafted acrylonitrile-butadiene-styrene
MA	Maleic anhydride grafted polyethylene
PP-g-MAH	Maleic anhydride-grafted polypropylene
m-BNRs	Modified boehmite nanorods
MMT	Montmorillonite
MWCNTs	Multiwalled carbon nanotubes
NC	Nanoclay
NR	Natural rubber
PTW	*n*-butyl acrylate glycidyl methacrypoles terpolymer
NBR	Nitrile rubber
phr	Parts per hundred
ABS	Poly(acrylonitrile-butadiene-styrene)
PB	Polybutylene
PBAT	Poly(butylene adipate-co-terephthalate)
PBS	Poly(butylene succinate)
PBT	Poly(butylene terephthalate)
PA	Polyamide
PA6	Polyamide 6
PA1010	Polyamide 1010
PCL	Poly(caprolactone)
PC	Polycarbonate
PDeF	Poly(decamethylene 2,5-furandicarboxylate)
PE	Polyethylene
PEG	Polyethylene glycol
PEO	Poly(ethylene oxide)
EVA	Poly(ethylene vinyl acetate)
POSS	Polyhedral oligomeric silsesquioxanes
PHAs	Polyhydroxyalkanoates
PLA	Poly(lactic acid)
PMMA	Poly(methyl methacrylate)
PO	Polyolefin
PPE	Poly(p-phenylene ether)
PPO	Polyphenylene oxide
PP	Polypropylene
PTT	Poly(trimethylene terephthalate)
PS	Polystyrene
PU	Polyurethane
PVAC	Poly(vinyl acetate)
PVC	Polyvinylchloride
PVDF	Poly(vinylidene fluoride)
PHP	Poly(vinylidene fluoride-hexafluoropropylene)
PHB	Poly(3-hydroxybutyrate)
p-BNRs	Pristine boehmite nanorods
PBE	Propylene based elastomer
rGO	Reduced graphene oxide
RHF	Rice husk flour
SEM	Scanning electron microscopy
SANS	Small angle neutron scattering
SAN	Styrene acrylonitrile
SBS	Styrene-butadiene-styrene rubber
SMA	Styrene maleic anhydride
SiO_2-PST	Surface modified SiO_2
TP	Thermoplastic
TPE	Thermoplastic elastomer
TPS	Thermoplastic starch
TS	Thermosetting
TEM	Transmission electron microscopy
UCST	Upper critical solution temperature
WAXS	Wide angle X-ray scattering
TMI	3-isopropenyl-α,α' -dimethylbenzyl isocyanate

be manufactured and stored. These factors explain why about 36% of the polymers are applied in blends and about 39% in composites. About 65% of polymer alloys are developed by polymer manufacturers, 25% by compounding companies and the other 10% by the transformers [2]. Generally speaking, five different manufacturing processes, i.e., melt compounding, solution blending, latex mixing, partial block or graft copolymerization and synthesis of interpenetrating polymer networks, can be utilized to produce these blends. The mixing of the blend components in the molten state through melt compounders such as screw extruders is by far the most diffused transformation technology of polymer alloys, because of the use of well defined components and of the versatility of the mixing devices [7].

Even if the blending technology represents an effective and economic way to obtain multifunctional high performances materials, it has to be considered that polymer alloys are often characterized by a coarse phase morphology and limited interfacial adhesion between the components, as most polymer pairs are immiscible [8]. In immiscible blends, coarse particles of the minor component are not homogenously distributed and have a poor adhesion with the surrounding matrix. More generally, when the miscibility conditions of polymer alloys are considered, a homogeneous mixture at the molecular level or a heterogeneous blend with distinct phases can be developed. According to the definitions provided by Utracki [9], a miscible blend is a mixture of two or more amorphous matrices homogeneous up to the molecular level,

satisfying thus the thermodynamic miscibility conditions of multicomponent systems. Conversely, thermodynamic phase stability conditions are not satisfied in immiscible blends. A compatible blend can be defined as an optically homogeneous polymer mixture, with better properties with respect to their components and with an elevated commercial potential. The thermodynamic equilibrium conditions of a miscible polymer mixture are reported in Equations (1) and (2) [10,11]:

$$\Delta G_{mix} = \Delta H_{mix} - T \cdot \Delta S_{mix} < 0 \quad (1)$$

$$\mu_i' = \mu_i'' = 1, 2, ..., n \quad (2)$$

where ΔG_{mix}, ΔH_{mix}, and ΔS_{mix} are respectively the Gibbs energy, enthalpy, and entropy of mixing of a polymer alloy formed by i components, while $\mu_i'$and μ_i'' are the chemical potentials of the component i in the phase μ' and μ''. The phase stability condition, reported in Equation (3), can be obtained for an incompressible polymer mixture:

$$\frac{1}{N_1 v_1} + \frac{1}{N_2 v_2} - 2\chi_{12} \geq 0 \quad (3)$$

where N_1 and N_2 are respectively the number of segments of component 1 or 2, v_1 and v_2 are respectively the volume concentration of component 1 and 2, and χ_{12} represents the interaction parameter between the two components. The first and second terms of Equation (3), denoting the entropy contribution supporting the blend miscibility, tend to zero (N_1, N_2 >> 1), and the miscibility is therefore regulated by the entalphic contribution, i.e., by the interaction parameter χ_{12}. In non-polar polymers with elevated molecular weight, a positive value of χ_{12} leads to a very limited miscibility, while a negative χ_{12} value is related to a homogeneous polymer alloy. In many cases it is difficult to determine the Huggins-Flory binary interaction parameter (χ_{12}), because highly viscous polymers diffuse very slowly to reach an equilibrium state. Moreover, the heat generated during the mixing operations can increase the temperature of the system, leading also to the partial thermo-mechanical degradation of the alloy [2]. Interaction parameter values for non polar polymers can be found in literature or determined through the expression reported in Equation (4):

$$\chi_{12} \approx (\delta_1 - \delta_2)^2 \quad (4)$$

where δ_1 and δ_2 represent the solubility parameters of the components [5]. Knowing that χ_{12} values are noticeably affected by the temperature, it is possible to determine the phase diagram of polymer alloys, drawing also the binodal and spinodal curves [12]. In Fig. 1 a representative phase diagram of a polymer mixture is reported. The area of instability of the blend, where phase separation is controlled by a spinodal mechanism, lies below the spinodal curve, while in metastable region, i.e., between spinodal and binodal curves, phase separation is controlled by a nucleation mechanism. The tangent points of binodal and spinodal curves define the upper critical solution temperature (UCST) and the lower critical solution temperature (LCST). In the review of Horak et al. it is possible to find a detailed description of these curves [5].

In Fig. 2 an example of morphology evolution in an immiscible polymer blend at different relative concentrations, constituted by a poly(butylene adipate-co-terephthalate) (PBAT)/poly(lactic acid) (PLA) alloy, is reported [13]. At a general level, evident phase separation can be detected in all the compositions, with a morphology constituted by a continuously interdispersed 3D network, or by discrete spherical domains dispersed within the polymer matrix (sea-island microstructure). The morphology of the PBAT/PLA

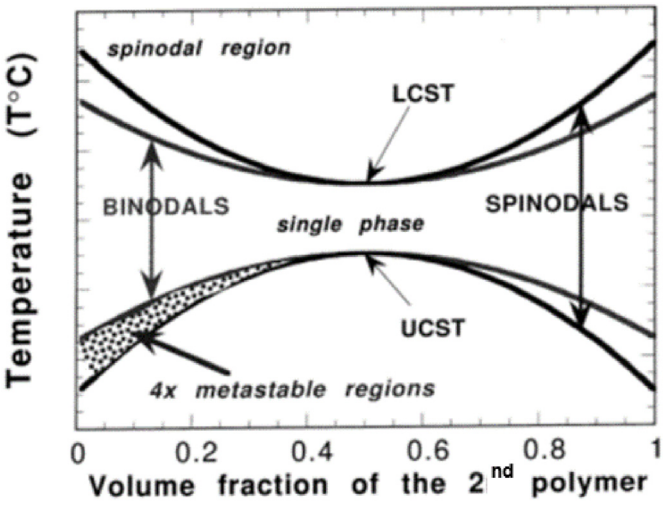

Fig. 1. An example of the typical phase diagram in a polymer blend (adapted with permission from Ref. [12]).

blend with a relative weight ratio 10/90 is characterized by small domains of PBAT, around 1 μm in size, dispersed within the PLA matrix. The diameter of PBAT spherical domains is very small, because the melt viscosity of PBAT is lower than that of PLA, and PBAT phase can be broken down into small droplets at the molten state. The micrograph of the 20/80 composition is typical of two interpenetrating phases, very similar to a co-continuous morphology, and also 30/70 and 40/60 blends present co-continuous phase microstructures. The coarsening of the structure detected in the 40/60 blend indicates that this composition is near the upper limit of the co-continuous range. With a PBAT/PLA ratio of 60/40 PBAT becomes the continuous phase, with dispersed droplets of PLA having size in the range 20–40 μm. The relatively big diameter of PLA domains for this composition can be explained by the difference in melt viscosity of the two components. Molten PLA droplets, having elevated melt viscosity, are not easily broken down and dispersed in the PBAT matrix. However, by increasing the PBAT concentration up to 80 wt%, a substantial refinement of the microstructure can be detected. It is also important to underline that in other blend systems the co-continuous microstructure can be substituted by a droplet-within-droplet (i.e. salami-like) [14] or by a ribbon like or stratified morphology [15].

Considering that the investigation of the morphological aspects is of utmost importance for the comprehension of the physical properties of the resulting blends, electron microscopy techniques, like scanning electron microscopy (SEM) and transmission electron microscopy (TEM), are widely utilized. They are very useful to determine the shape and the size of the domains within the blends, and the extent of their interfacial adhesion with the major component. With SEM it is also possible to correlate the evolution of the morphology to the processing parameters applied. In order to perform a more comprehensive investigation of the physical properties of polymer alloys, it is important to combine different techniques, like wide angle X-ray scattering (WAXS), small angle X-ray scattering (SAXS), small angle neutron scattering (SANS), light scattering (LS) and differential scanning calorimetry (DSC) [5]. It is also important to underline that the utilization of theoretical models and numerical simulations to predict the physical properties of a blend can represent an interesting way to save time and costs when a new polymer alloy must be developed, even if it cannot fully replace the experimental investigation activities [4].

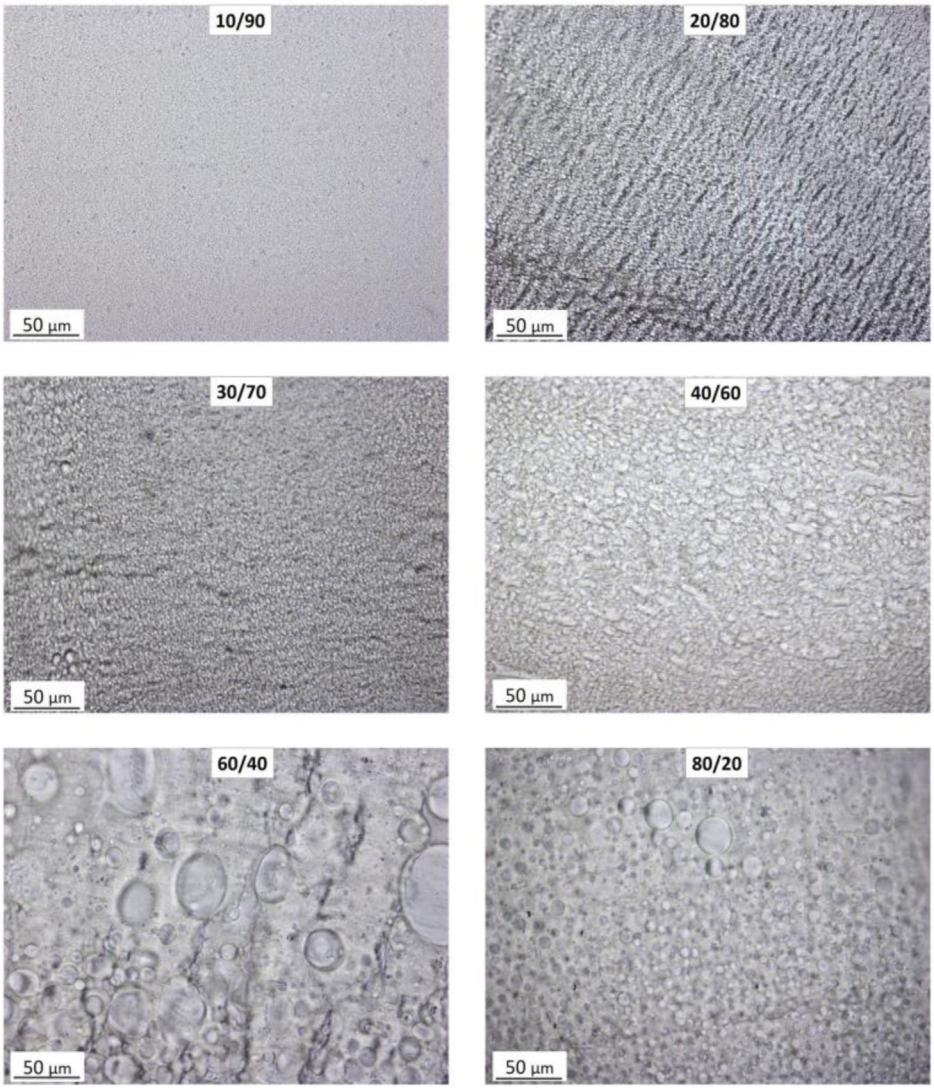

Fig. 2. Evolution of the phase structure as a function of the relative composition in PBAT/PLA blends (reprinted with permission from Ref. [13]).

Considering that miscibility in polymer alloys can be achieved only through a specific combination of conditions (i.e., molecular weight and molecular weight distribution of polymeric phases, temperature, stress field, additives, etc.), the greatest part of the commercial blends is immiscible. Moreover, considering that the macroscopical properties of polymer alloys are strictly dependent by their morphology, this means that their microstructural features must be stable, not strongly affected by the processing conditions, reproducible and easily predictable [3]. Therefore, compatibilization is the most widely utilized technique to obtain these effects [16,17]. Compatibilization is generally performed (i) to decrease the interfacial tension and thus to obtain a finer dispersion of the minoritary component, (ii) to limit the effects on the morphology played by thermo-mechanical stresses applied during the processing at the molten state, (iii) to increase the interfacial adhesion between the phases, improving thus the mechanical properties of the resulting alloys [3]. Several strategies of compatibilization have been proposed in literature in the last decades, and in the following Chapter the most commonly adopted approaches will be described.

2. Compatibilization of polymer blends

As already mentioned in Chapter 1, the processing of polymer alloys through simple melt mixing leads to the development of materials that are generally characterized by evident phase separation, with coarse domains of the minoritary component having poor interfacial adhesion with the surrounding matrix. In these conditions the physical features, and in particular the mechanical properties, of the resulting blends will be unsatisfactory. Compatibilization is therefore required to face these problems, with the aim to obtain a stable microstructure, characterized by a finer phase dispersion and better adhesion between the components, thanks to a reduction of the interfacial tension. A schematic representation of the role played in immiscible blends by the compatibilization, performed through the addition of a compatibilizer, is reported in Fig. 3.

Generally speaking, compatibilization is the creation of physical or chemical bonds between the blend phases through the addition of a component, called compatibilizer [18]. Polymer blends can be compatibilized by applying different approaches, and the suitability

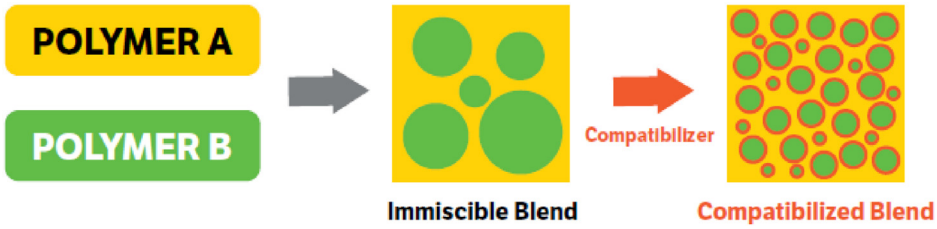

Fig. 3. Schematic representation of the effect of the addition of a compatibilizer in a biphasic immiscible polymer blend.

of a compatibilization technique at the industrial level is strongly related to many aspects, such as cost, final performance, recyclability, and possible biodegradability. According to the review of Ajitha et al. the following compatibilization strategies (other than the simple mechanical mixing at the molten state) can be considered [8].

- adding block or graft copolymers
- adding reactive polymers
- addition of low-molecular-weight chemicals
- utilization of interchange reactions
- adding selective crosslinking agents.

Besides traditional compatibilization techniques, some novel approaches have recently emerged. Among them, the addition of solid micro- and nanofillers as compatibilizers is a very promising possibility, especially when a limited filler amount is required. This is the approach that will be extensively described in the present review, with particular focus on the role played by the nanofillers on the blends compatibilization. In the following Paragraphs, a general description of the two most frequently used compatibilization techniques, i.e., insertion of block or graft copolymers and reactive compatibilization, will be reported, together with the presentation of the role played by fillers addition on the compatibility of polymer alloys.

2.1. Compatibilization through the addition of block and graft copolymers

The most widely utilized compatibilization technique is based on the addition to the two immiscible components of a third polymeric component, either a block or graft copolymer, having often identical or similar chain segments to those of the main polymers. It is important that the segments of these copolymers are able to establish specific interactions with the two polymer components, such as hydrogen bonding, dipole-dipole, dipole-ionic, Lewis acid-base, etc. In order to be effective, this compatibilizer should be able to migrate at the interface, in order to modify the rheological behavior and reduce the interfacial tension of the blend [3]. In this way, the morphology of the resulting alloy will be stabilized and the coalescence of the domains of the minoritary component will be strongly reduced (see Fig. 4) [19], with a consequent improvement of the physical properties [20]. The microstructural features and the performances of the resulting materials will be also strongly related to other factors, such as the adopted processing conditions, the relative concentration of the blend components and the copolymer structure [5]. In order to achieve effective compatibilization, the copolymer should have elevated miscibility with both the polymeric components of the alloy, limited molecular weight (i.e., just about the entanglement molecular weight for each interacting segment), and low concentration (0.5–2 wt%) in the blend [3].

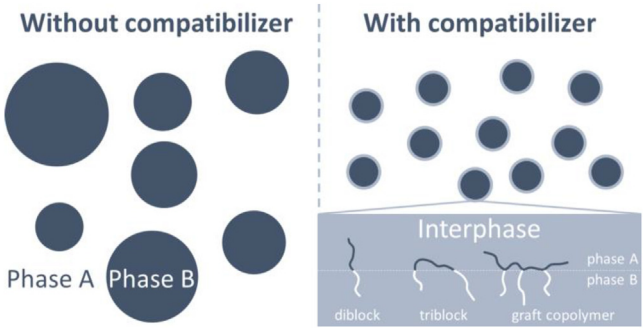

Fig. 4. Effect of the compatibilization on the morphology of polymer blends due to the activity of graft and block copolymers at the interface (reprinted with permission from Ref. [21]).

Among block copolymers, those based on styrene and butadiene have been widely applied, also because they have been the earliest discovered, while ethylene-propylene copolymers have been extensively adopted for the compatibilization of polyolefins [22]. For instance, a hydrogenated styrene-butadiene-styrene triblock copolymer (SEBS) was added as compatibilizer in polypropylene/polycarbonate (PP/PC) blends. In the formulations with a PC content of 10–20 wt% and a PP/SEBS weight ratio of 95/5 to 90/10, SEBS was able to envelop PC drops embedded in PP, due to better interfacial affinity of SEBS to PP than that present between PC and PP [23]. The interfacial compatibilization efficiency of hydrogenated butadiene-b-styrene (SEB) and hydrogenated butadiene-b-isoprene-b-styrene (SEP) copolymers in polyethylene/polystyrene (PE/PS) blends has been investigated by Fayt et al. [24–26]. It was shown that the copolymers were present at the interface, forming a continuous layer around the minoritary component, either PE in PS or PS in PE, with a thickness similar to the radius of gyration (10–12 nm). In particular, a SEB loading of 2–5 wt% was able to decrease the interfacial tension coefficient and the coalescence tendency, increasing thus the mechanical properties [24,25]. In a paper of Lee et al. a maleic anhydride-grafted polypropylene (PP-g-MAH) compatibilizer was added to polypropylene/poly(acrylonitrile-butadiene-styrene) (ABS) blends, prepared through a twin-screw extruder with a PP/ABS ratio of 70/30 wt%. Fig. 5(a–d) reports the SEM micrographs of this blend with PP-g-MAH contents from 0 to 5 parts per hundred (phr). An increase in the concentration of compatibilizer led to an evident refinement of the microstructure, the ABS domain size decreased from 18 to 7.5 μm, and tensile strength was correspondingly enhanced (from 36 MPa to 40.5 MPa) [27]. Similar results have been found also by other researchers on PP/ABS blends compatibilized with block or graft copolymers. Even in these works, the amount of compatibilizer played a key role on the physical properties of the resulting blends [28].

Also graft copolymers are very often utilized as compatibilizers. In a paper of Zhang et al. the compatibilization efficiency of graft

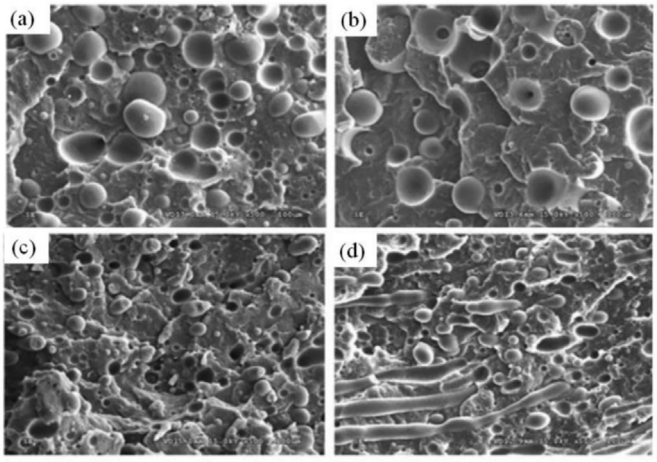

Fig. 5. SEM images of PP/ABS blends (70/30 wt%) with a PP-g-MAH compatibilizer amount of (a) 0, (b) 1, (c) 3, and (d) 5 phr (reprinted with permission from Ref. [27]).

copolymers and the influence of the feeding mode on the compatibilization capability were investigated through the emulsification curve approach, that describes the evolution of the dispersed phase size with the copolymer concentration [29]. In this paper the blends were composed of PS (the matrix) and polyamide 6 (PA6, the dispersed phase). A series of graft copolymers of PS and PA6, denoted as PS-g-PA6, with different molecular structures were used as compatibilizers. Feeding mode significantly affected the dispersed domains size at short mixing time, while its effect decreased or became negligible at long mixing time. Also the molecular structure of the PS-g-PA6 graft copolymer had a strong influence on the compatibilization of these blends. Moreover, at a fixed emulsifier/dispersed phase relative concentration, the size of the PA6 droplets increased with the PA6 amount, because of coalescence phaenomena. In a similar paper of the same research group, a series of PS-g-PA6 graft copolymers with different molecular structure were used to compatibilize PS/PA6 blends with different relative compositions [30]. PS-g-PA6 was more efficient for the PS/PA6 (80/20 wt%) blend than for the PS/PA6 (20/80 wt%) one, meaning that a graft copolymer whose backbone and grafts matched the matrix and the dispersed phase polymers, respectively, had higher compatibilizing efficiency. Moreover, for PS-g-PA6 graft copolymers with the same backbone and the same number of grafts per backbone, the compatibilization effect increased with the grafts length. For a given backbone/graft mass ratio, the compatibilizing efficiency of the graft copolymer increased reducing the number of grafts per backbone (i.e., increasing the graft length).

2.2. Reactive compatibilization

In the reactive compatibilization method, graft or block copolymers are directly generated in situ during melt blending, and utilized as compatibilizers. Thanks to chemical reactions between properly functionalized polymers, with this technique it is possible to synthesize the copolymers at the blend interface, and the immiscible phases will be directly linked through covalent or ionic bonds. This will lead to a refinement of the dispersed phase and to an increase in the interfacial adhesion. This approach is based on a complex integration between organic chemistry and polymer processing, in which the aspects of the chemical kinetics are connected with the rheological and thermal properties of the reaction ingredients and products [3]. By using reactive compatibilization, the difficulties related to the transport of the compatibilizer to the interface are overcome, and this leads to a better control of the blend microstructure with respect to the addition of preformed copolymers. In an efficient reactive compatibilization, the reactions between the functional groups should be selective and fast, and the mixing conditions should minimize the limitation of mass transfer during the reaction [5]. Another positive aspect of the reactive compatibilization is that the molecular weight of each of the two distinct polymeric segments in the copolymer is about the same that the corresponding polymer phase in which the segment must dissolve, and this will lead to an optimization of the interfacial adhesion [2]. Moreover, with reactive blending it is possible to obtain a thicker and more rigid interphase than blends with added copolymer. For instance, the interfacial thickness in alloys of amorphous polyamide (PARA) with a styrenic copolymer, either styrene maleic anhydride (SMA) or styrene acrylonitrile (SAN), was measured through a time-resolved ellipsometric method during annealing [31,32]. An increase of the interphase thickness with time was observed, until reaching a plateau, whose value (between 10 and 60 nm, i.e., larger than the radius of gyration of the copolymer) was related to the temperature and concentration of the reactive sites [33].

Generally speaking, for the reactive blending in an extruder five groups of chemical reactions can be performed: (i) chain cleavage and recombination, (ii) end group of first polymer reacting with end group of second polymer, (iii) end group of first polymer reacting with pendant functionality of second polymer, (iv) covalent crosslinking between reactive groups of two polymers that are parts of either main or side polymer chains, (v) ionic bond formation [3]. Reactive functional groups such as anhydride, hydroxy, amine, or carboxy are thus incorporated into one or both the components to be compatibilized. For instance, an effective reactive compatibilization can be performed if maleic anhydride-grafted PP, PE, ethylene propylene rubber (EPR), ethylene propylene diene monomers (EPDM), SEBS or ABS react with polymers with aminic functionalities [34,35]. Reactive compatibilization can be also carried out by introducing low molecular weight compounds [35], by combination of a peroxide with an oligomer coagent in PE/PP blends [36] or bis-maleic imide in PE/poly(butylene terephthalate) (PBT) alloys [37]. Moreover, radical initiated reaction of monomers forming homopolymers and grafts on the chains of dissolved polymers, that is the method used for the synthesis of high impact polystyrene (HIPS) or ABS, can be intended as a special case of reactive compatibilization [38]. In the books of Utracki, it is possible to find an overview of the most widely utilized polymer blends produced through reactive compatibilization [2,3]. For instance, super-tough polyamide (PA), polyolefin (PO)/PA and poly(p-phenylene ether) (PPE)/PA blends, or PC/PA alloys are nowadays produced through reactive processing. With this technique, it is possible not only to generate new blends, but also to develop traditional blends with novel and peculiar properties, like in the case of polymer alloys with specialty resins, or new polyvinylchloride (PVC)/acrylics systems.

The first stage of the reactive compatibilization is often based on the modification of a polyalkene resin, usually performed through grafting it with either maleic anhydride or glycidylmethacrylate. These reactions can be promoted by the introduction of styrene into the reacting medium [39]. As an example, maleation of PP followed by compounding with polyamide 6 (PA6) was performed in a twin-screw extruder, and the average size of the dispersed PA6 domains decreased with the concentration of the generated di-block copolymer from 20 μm to 0.14 μm (with a copolymer amount of 20 wt%). In a recent paper of He et al. PET/propylene-based elastomer (PBE) blends were prepared through a novel elongational rheology extruder, by using an ethylene/

methylacrylate/glycidyl methacrylate copolymer (EGMA) as reactive compatibilizer, selectively localized at the interface [40]. With an EGMA concentration of 6 wt% an increase of the impact strength up to 35 kJ/m^2, about seven times higher than that of the uncompatibilized blend, was detected. Furthermore, the tensile strength and elastic modulus of the compatibilized blend were only decreased by 10% and 13%, respectively, compared to the uncompatibilized alloy (see Fig. 6). Thanks to Fourier-transform infrared (FT-IR) spectroscopy and rheological characterization, it was possible to ascribe the observed improvement of the mechanical performances in the compatibilized blend to the interfacial reactive compatibilization between PET and PBE, i.e., to the in-situ reaction between carboxyl or hydroxy group of PET and epoxy group of EGMA, and to the consequent morphology refinement.

Another approach that has been recently applied in the industry refers to a reactive compatibilization technology that leads to the formation of nanoblends. Common polymer blending methods do not lead to nano-structured polymer blends and it is impossible to disperse one polymer in another at a scale smaller than 100 nm, unless both polymers are miscible enough. In the nanoblends approach the monomer of polymer A is directly polymerized in polymer B, while generating an in situ compatibilization. In this way, it is possible to obtain nanoblends, in which one polymer is dispersed in another at a scale smaller than 100 nm. For instance, Hu et al. prepared PP/PA6 nanoblends in a screw extruder polymerizing a monomer of PA6 (ε-caprolactam) in the PP matrix [41]. A fraction of 3-isopropenyl-R,R-dimethylbenzene isocyanate acted as growing centers to initiate PA6 chain growth. In this way, it was possible to simultaneously synthesize PA6 and a graft copolymer of PP and PA6 in the PP component, leading to compatibilized PP/PA6 blends in which the diameter of the PA6 droplets was between 10 and 100 nm. In the following papers of the same research group, the kinetics of the PA6 polymerization and of the in situ compatibilization in these blends was comprehensively investigated [42,43].

A novel reactive compatibilization technology which has recently gained more importance is based on the use of modified vegetable oils, derived from renewable sources. In the last years, this compatibilization technique has been applied both in immiscible polymers [44–47] and for improving the interfacial adhesion between fillers and matrix [48–51]. In the case of polymer blends, vegetable oil compatibilizers were mainly applied to improve the physical properties of bioplastic alloys based on polylactic acid (PLA). For instance, in a paper of Carbonell-Verdu et al. the reactive compatibilization of PLA/PBAT blends (80/20 wt%) was perfomed by using different amounts (from 1 to 7.5 wt%) of epoxidized and maleinized cottonseed oil [44]. It was found that the addition of maleinized cottonseed oil at a concentration of 7.5 wt% led to a remarkable increase in the elongation at break up to values over 320% with respect to neat PLA, keeping the elastic modulus and the tensile strength at high levels. In a paper of Garcia-Campo et al. a ternary blend of PLA, poly(3-hydroxybutyrate) (PHB) and poly(caprolactone) (PCL) with fixed relative concentration (60/10/30 wt%) was compatibilized with epoxidized soybean oil, maleinized soybean oil and acrylated epoxidized soybean oil [45]. All three soybean oil-based compatibilizers led to a noticeable increase in toughness, while both the tensile modulus and strength decreased, but in a lower extent with respect to common plasticizers. This compatibilizing effect was explained considering the reaction between the terminal hydroxyl groups in all the three biopolyesters (PLA, PHB and PCL) and the readily reactive groups in the soybean oil derivatives, i.e., epoxy, maleic anhydride and acrylic/epoxy functionalities. In a recent paper of Hu et al. PLA/starch blends were prepared through reactive melt blending by using polyethylene glycol (PEG) and citric acid (CA) as compatibilizers [46]. It was shown that the elongation at break and impact strength of the compatibilized blend were 13.4 and 1.8 times higher than those of neat PLA, respectively, thanks to the esterification reaction between CA, PEG, and starch during melt blending. Quiles-Carrillo et al. investigated fully bio-based blends of polyamide 1010 (PA1010) with 20 wt% of PLA, reactively compatibilized with two multi-functionalized vegetable oils (i.e., maleinized linseed oil and epoxidized linseed oil) and two petroleum derived glycidyl-based additives (i.e., epoxy styrene-acrylic oligomer and styrene-glycidyl methacrylate copolymer) [47]. Although all four compatibilizers successfully provided compatibilization to the blends, the samples compatibilized with modified vegetable oils highlighted the most balanced mechanical properties in terms of strength and toughness and very low oxygen transmission rate values.

2.3. Compatibilization induced by the addition of micro- and nanofillers

The interest in the introduction of fillers in polymer blends is continuously increasing, and nowadays filled polymer alloys find widespread application in many industrial sectors [17]. This Paragraph is focused on the compatibilization effect promoted by the addition of solid fillers (both micro- and nanostructured) in polymer blends.

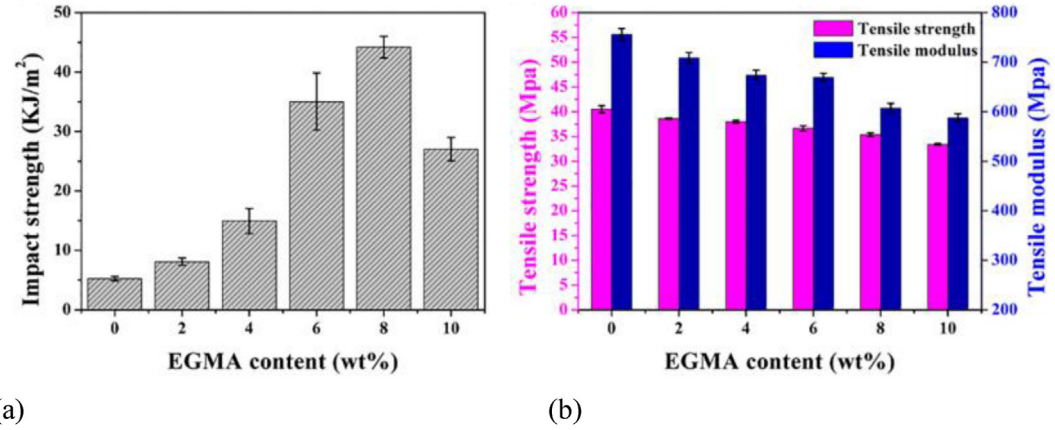

Fig. 6. Mechanical properties of reactively compatibilized PET/PBE blends. (a) Impact strength, (b) tensile strength and tensile modulus as a function of the EGMA content (reprinted with permission from Ref. [40]).

Even if the introduction of nanofillers in blends is attractive both from a technical and economical point of view, also because a limited filler concentration is required, in literature it is possible to find many examples on the compatibilizing action promoted by microfillers in polymer alloys. Shifrin et al. reported a systematic investigation on the localization of a mineral microfiller utilized as compatibilizer in a biphasic blend, based on the analysis of the interaction between the filler and individual polymer components [52]. If the filler presents a similar affinity to each polymer phase, it will be located in the interfacial region, otherwise it will concentrate in the component where the interaction is stronger. Karim et al. investigated the role played by the addition of fumed silica particles on the phase stability of a polystyrene/polybutylene (PB) blend. It was found that the upper critical solution phase boundary of this alloy was destabilized by the introduction of untreated fumed silica, while the cloud point temperature of this blend was decreased or became stabilized upon the addition of surface treated fumed silica, with important consequences on the properties of the resulting blends [53].

The effect of untreated silica on the phase boundaries and on the Flory-Huggins interaction parameter (χ) of poly(methyl methacrylate) (PMMA)/SAN blends were investigated by dynamic shear rheological tests. It was found that the addition of silica to this polymer alloy led to a substantial increase in the phase stability, with an increase in the phase separation temperature and a corresponding decrease of the χ parameter over the whole range of investigated temperature (see Fig. 7(a and b)). These results were explained considering that the adsorption of high molecular weight fraction of PMMA macromolecules on silica surface decreased the average molecular weight of PMMA in the matrix, promoting thus its miscibility with the SAN phase [54]. Ishida et al. studied the compatibilization effect played by glass beads (both silane treated and untreated) on an immiscible nylon 6/polypropylene blend [55]. The presence of the filler and of the surface treatment changed the rheological properties and the main relaxation behavior of the blend. Moreover, the addition of glass beads played an important role on the interphase structure, modifying the crystallinity, adhesion and morphology behavior of the blend.

In the last decades, polymer nanocomposites attracted the attention of both industries and academia, as the physical, mechanical, thermal, and electrical properties of engineering plastics could be strongly modified upon the introduction of limited concentrations of nanostructured materials (up to 5 wt%). Therefore, nanocomposites have recently found wide application in automotive, medical, aerospace, sports, recreation, and renewable energy sectors [56]. Nanocomposites are defined as composite materials in which nanometric fillers, having at least one dimension below 100 nm, are introduced [57]. Generally speaking, nanofillers can be classified according to their shape into three categories (see Fig. 8).

- monodimensional nanofillers, like layered silicates and graphite nanoplatelets (GnP)
- bidimensional nanofillers, like carbon nanotubes (CNTs) or nanofibers, boron/nitrogen nanotubes, MoS_2 and WS_2 nanotubes, V_2O_5, and MoO_3 nanotubes, and organic nanotubes
- three-dimensional nanofillers, like metal oxides nanoparticles (ZnO, SiO_2, Al_2O_3, $CaCO_3$, TiO_2), silicon carbide (SiC) and carbon black (CB) nanoparticles, polyhedral oligomeric silsesquioxanes (POSS).

The dispersion and/or distribution of the nanofiller within the hosting polymer and the filler/matrix interaction determine the physical properties of the resulting composites. In fact, the behavior of the macromolecules in contact with nanostructured materials is substantially different than that shown in bulk matrices, as nanocomposites are characterized by a very large interfacial area.

For as concerns polymer alloys, the addition of nanofillers to tailor their properties represents an interesting possibility to develop high performance multifunctional materials [58]. In particular, nanofillers can be used as compatibilizers or nucleating agents to stabilize the blend morphology and to obtain a substantial improvement of the mechanical, thermal, chemical properties. It is important to underline that the performances of nanocomposite polymer alloys are strongly affected by the chemical nature of the components, by the blend morphology, by the dispersion, localization and orientation of the nanofiller within the matrix. Many papers in literature highlighted the compatibilization effect on polymer blends provided by the introduction of both unmodified and surface treated nanofillers. It has to be considered that the use of untreated nanoparticles should be preferred when elevated processing temperatures are required, in order to avoid the thermal degradation of the organic modifier [8]. Both the surface area and the aspect ratio of the nanofiller play a key role in the compatibilization of the resulting alloys, as it was demonstrated that fillers with elevated aspect ratio can more effectively reduce the size of the dispersed domains [59].

There are some complex thermodynamic theories dealing with the analysis of the factors that determine the compatibilizing action promoted by nanofillers in polymer blends, and the role played by nanostructured materials on the phase separation has been mainly

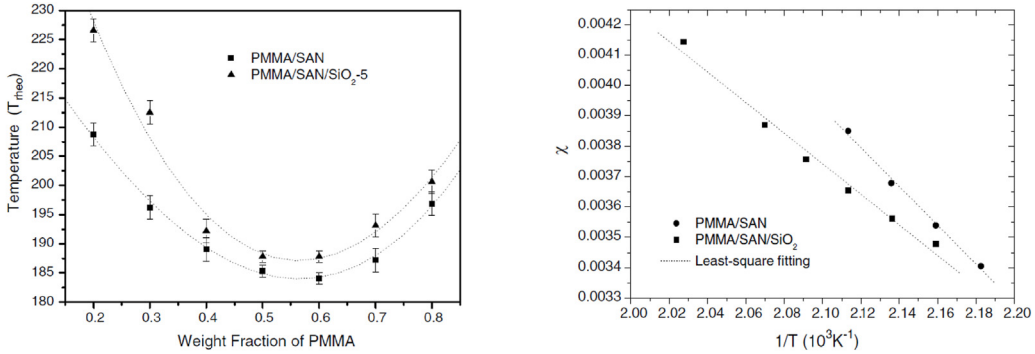

Fig. 7. (a) Phase diagrams determined by shear rheology and (b) temperature dependence of the interaction parameter of PMMA/SAN/SiO_2 (silica content = 5 wt%) and PMMA/SAN blends (reprinted with permission from Ref. [54]).

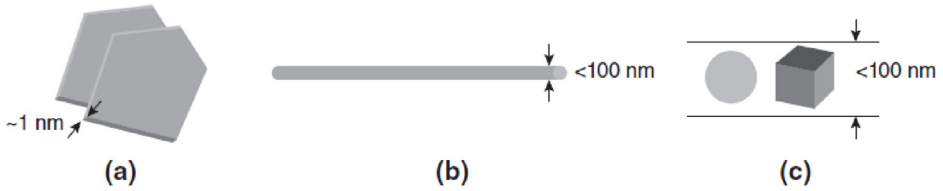

Fig. 8. Dimensional classification of nanofillers: (a) plate-like materials, (b) nanotubes, and (c) equiaxed nanofillers (adapted with permission from Ref. [57]).

investigated by Lipatov, Nesterov [60], and Ginzburg [61]. However, a detailed description of these theories is out of the main scope of this review. Generally speaking, compatibilization in nanocomposite blends can be explained through the selective localization of the nanofiller, that leads to a decrease of the interfacial tension, to a suppression of the coalescence tendency and to a morphology refinement [62]. All these effects are considered in the Taylor theory [63], and the correlation between interfacial tension (σ_{int}), viscosity of the matrix (η_m), and shear rate (γ') with the resulting domain size (d) can be expressed as reported in Equation (5):

$$\sigma_{int} = \frac{\eta_{m \cdot \dot{\gamma} \cdot d}}{W_c} \quad (5)$$

where W_c is the Weber number. According to this Equation, a decrease of the dimension of the dispersed domains leads to an increase in the interfacial area, to a lower interfacial tension and thus to a better interaction between the components, with a consequent improvement in the performances of the blend. If the selective location of the nanofiller plays a key role on the compatibilization of polymer alloys, the refinement of the blend morphology is related to two different mechanisms. If the nanostructured materials are preferentially located in any one of the phases of the blend, they can generate a percolative network, with a consequent viscosity increase that hinders the coarsening of the dispersed domains (Fig. 9(a)). On the other hand, if the nanofiller is localized at the interface, the reduction of the coalescence tendency is due to the trapping action played by the nanoparticles at the interface (Fig. 9(b)) [8].

It has been demonstrated that the localization of the filler in nanocomposite blends strongly depends on filler/polymer, filler/filler, and polymer/polymer interaction [64], and it is also affected by the aspect ratio of the nanofiller [65]. In literature it was shown that the localization of high aspect ratio fillers (like CNTs, graphene, etc.) in the interfacial region is very difficult, as large aspect ratio nanoparticles are characterized by an elevated migration rate across the interface and present low stability in the interface. On the contrary, low aspect ratio nanofillers (like CB) are mainly located in one phase of the blend. The degree of migration of the nanofillers between the two phases of a nanocomposite blend is related to thermodynamic factors, while their migration rate is determined by kinetic parameters, like the viscosity of the blend components, the applied shear rate, and the mixing time [66]. Referring to the classical thermodynamics theory (i.e., Young's equation) [67–69], it is possible to predict the selective localization of nanofillers in polymer alloys, on the basis of the interfacial energy values and the wetting coefficient (ω_a), as reported in Equation (6):

$$\omega_a = \frac{\gamma_{A/F} - \gamma_{B/F}}{\gamma_{A/B}} \quad (6)$$

where $\gamma_{A/F}$ is the interfacial energy between polymer A and filler F, $\gamma_{B/F}$ is the interfacial energy between polymer B and filler, and $\gamma_{A/B}$ represents the interfacial energy between the two polymer phases. If $\omega_a > 1$ the filler will be preferentially located in polymer B, if $\omega_a < -1$ it will be localized in polymer A, if $-1 < \omega_a < 1$ the nanofiller will be present in the interfacial region [70,71]. In literature several works dealing with the nanofiller localization in polymer blends can be found [72–76]. For instance, Zhang et al. investigated the morphological features of poly(ethylene vinyl acetate) (EVA)/thermoplastic polyurethane (TPU)/multiwalled carbon nanotubes (MWCNTs) nanocomposite blends [77], predicting that MWCNTs would be preferentially dispersed within the TPU phase on the basis of the determination of the wetting coefficient. From the TEM micrographs reported in Fig. 10(a and b), it is possible to see that this theoretical prediction was well matched with experimental observations.

It has also to be considered that the incorporation of nanofillers within polymer blends can substantially affect their crystallization behavior, with important consequences on the morphology, on the compatibility between the components, and on the mechanical properties. As reported in the review of Das et al. on the crystallization in nanocomposite blends, depending on the filler/polymer interaction, a new crystal may be generated in the proximity of nanostructured fillers, which may not be present in case of the unfilled polymer alloys, with direct influence on the performances of the resulting material [58].

Recently, also Janus nanoparticles have been proposed as a novel compatibilizer for polymer alloys. Janus particles are a particular kind of surface partitioned materials, characterized by different chemical compositions or physical properties on two sides of the same particle [78]. Janus nanoparticles combine the advantages of both amphipathic diblock copolymers and nanoparticles. In fact, they can effectively migrate to the interface due to the selective interaction with the two polymer components, and they can also stabilize the interface. Janus particles can refine the morphology and customize the interfacial properties of the blends, leading to

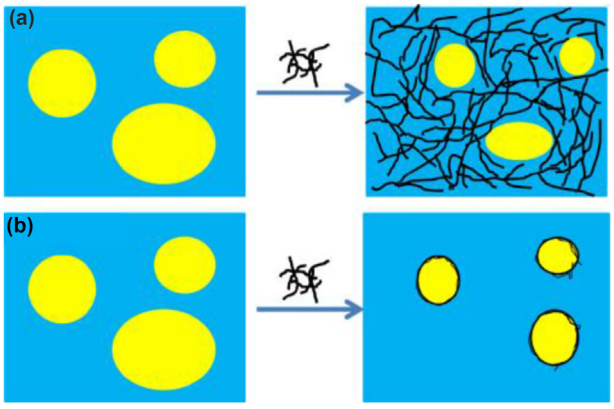

Fig. 9. Two main strategies of nanofiller induced compatibilization of polymer blends, based on the selective localization of the filler (reprinted with permission from Ref. [8]).

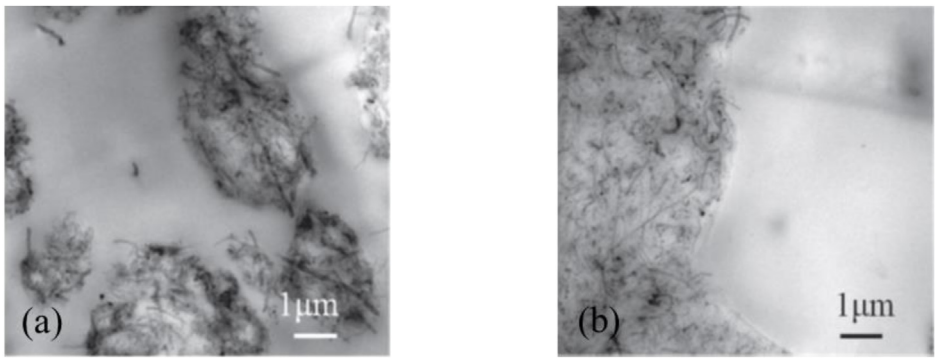

Fig. 10. TEM images of EVA/TPU/MWCNTs nanocomposites blends (CNT content = 5 wt%). EVA/TPU relative ratio of (a) 80/20 wt% and (b) 50/50 wt%. The dark portion indicates the TPU with MWCNTs (adapted with permission from Ref. [77]).

the development of multifunctional polymer alloys with enhanced mechanical properties [79]. A recent review of He et al. comprehensively described the state of the art of Janus particles for the compatibilization of polymer blends [80]. However, a detailed description of the compatibilizing action promoted by Janus nanoparticles in polymer alloys is out of the main scope of this review.

When the compatibilizing action provided by nanoparticles in polymer blends is considered, it has already been mentioned that the morphological features of the nanofiller (i.e., size, aspect ratio, aggregation state) and its surface chemistry strongly influence the blend microstructure, and therefore the resulting properties of the polymer alloy. Moreover, also the way in which the nanoparticles are synthesized can play a crucial role, render them suitable for some specific applications. In literature it is rather difficult to find a general consensus on the effect played by the nanofiller morphology and chemistry on the performances of the resulting blends [81]. However, in the review of Taguet et al. it was clarified that in these ternay systems the shape of the nanoparticles, the particle radius (R_p) versus the radius of gyration of the macromolecules (R_g), and the surface chemistry of the nanofiller are the most influential parameters for the determination of the particles localization and of the resulting mechanical, conductive, magnetic and thermal performances of the blends [82]. In the same review, it was highlighted that also a proper choice of the processing conditions is of utmost importance. In particular, it was shown that an increase of the average shear rate (i.e., of the mixing energy) during the compounding procedure led to a better exfoliation of lamellar nanofillers, changing the size of the dispersed phase, and the same effect could be obtained applying longer mixing time and higher rotation speed [83,84]. Some authors tried to vary the sequence of mixing of the polymer pairs with fillers, showing a strong effect of the order of addition on the final properties of the system. It is therefore clear that the kinetics of the particles transfer at the interface depends on the shear forces involved and on the rheology of each polymer component under the processing conditions [85].

For as concerns the effect of the nature of the nanofiller on the blend compatibilization, in the last years molecular dynamics simulation was extensively used to study the influence of the shape, volume fraction and size of nanoparticles on the morphological and mechanical properties of the blends [86]. Concerning the nanorods, it was shown that the morphology of the system depended strongly on the aspect ratio (AR) and the volume fraction (Φ) of the nanofiller. Full phase separation occurred if $2 \cdot AR \cdot \Phi < 3$, while microphase separation could be detected if $2 \cdot AR \cdot \Phi > 3.29$. Contrary to nanorods, nanospheres in immiscible fluids did not lead to microphase separation [87]. At a general level, there are two main effects of the nanofiller shape on the final properties of the blends, i.e., the specific surface area (and hence the AR), and the matrix/droplet interface saturation. When polymers are adsorbed at the surface of the inorganic filler, a large surface area per unit weight would lead to a large stabilizing energy gain [88]. Zhang et al. explained that, since nanoplatelets have a high aspect ratio and can deform and follow the interface, they can cover a large surface domain, whereas nanotubes and spheres cannot. Hence, to saturate the interface between matrix and droplets of immiscible polymer blends, nanoplatelets are the best candidate [89]. Moreover, Goldel et al. proved that high aspect ratio fillers could be transferred faster and more effectively with respect to low AR nanoparticles. This is due to the change of the blend interface curvature during the transfer process, and it explains the fast and complete transfer of high AR fillers (like CNTs) from a less favorable into a more favorable wetting blend phase [73].

Dispersion/aggregation of the nanoparticles is another key factor for the final morphology of nanofilled polymers and blends. It is well-known that polymer macromolecules are depleted at the surface of a solid, because the number of possible conformations is decreased (decrease of the configurational entropy). The particle size influences both the dispersion and the aggregation of the nanoparticles, and in systems where only entropic forces are considered, if $R_p/R_g < 1$, particles disperse uniformly and the system is stabilized, whereas if $R_p/R_g > 1$ particles aggregate, deteriorating thus the physical properties of the blend [90].

It is also clear that the surface chemistry of the filler can affect its dispersion in polymer blends, leading thus to different final properties. For instance, the use of different organic modifiers in organoclays could result in a different affinity with one or both the polymer components, changing the mechanical response of the resulting materials [91], while the surface coverage of nanoparticles by apolar molecules had an influence on the size of the dispersed phase and thus on the final mechanical properties [92]. In the last years, some authors started to synthesize new nanoparticles with highly controlled surface properties and structure and to control their localization and dispersion in polymer blends. It is clear that the choice of the synthesis conditions plays a key role on the morphology and the final properties of the polymer alloy, especially when novel nanofillers (i.e., Janus nanoparticles) or functionalized nanoparticles are considered [93].

However, the comprehension of the effect played by the mophological and chemical features of nanostructured materials on blend compatibilization is quite far from being complete, and a lot of efforts should be made in the future on this specific topic.

3. Effect of nanofiller addition on the compatibilization of polymer blends

As already mentioned in Paragraph 2.3, the compatibilization induced by nanofillers introduction in polymer blends may be ascribed to the increase in the viscosity of the phase in which the nanofillers are localized, to the development of a strong polymer/filler interaction, to the reduction of the interfacial tension, and also to possible changes in the crystallization behavior of the polymer components [8]. Therefore, nanofiller compatibilization of polymer alloys can be considered as the result of a complex interplay of both thermodynamic and kinetic effects, that can lead to a substantial morphology refinement and stabilization. In literature it is possible to find several studies focused on the compatibilization provided by nanofillers in polymer blends. In the following paragraphs, an overview of the compatibilizing effect generated by different nanofiller types on thermoplastic, thermosetting and elastomeric based blends will be reported.

3.1. Thermoplastic based polymer blends

The greatest part of the works present in literature on nanofiller induced compatibilization is related to thermoplastic polymer blends.

Hemmati et al. studied the compatibilization effect of organically modified nanoclay (NC) on PE/EVA blends exhibiting UCST behavior [94,95]. It was shown that, regardless of the relative ratio of the components, the introduction of intercalated NC shifted the phase transition temperatures to lower values, modifying also the symmetry of the phase diagram (see Fig. 11). Organoclay introduction led to better miscibility in the amorphous regions of these nanocomposite blends, producing a finer biphasic morphology, reducing the interfacial tension up to two orders of magnitude, and slowing the phase separation kinetics. Moreover, the compatibilizing and reinforcing action promoted by NC addition led to a substantial increase in the impact strength.

Polypropylene is one of the most interesting thermoplastics, due to its easy processability, versatility, and cheapness [96]. However, its application is often limited by its relatively poor impact strength, especially below the T_g (i.e., around 0/-10 °C). Blending PP with elastomers is a common approach to increase the impact toughness, at the expense of the stiffness and tensile strength. Therefore, nanofiller addition in these blends could represent an attractive solution to obtain a good balance of mechanical properties. In the work of da Silva et al. the morphological and thermo-mechanical features of polypropylene/styrene–butadiene–styrene rubber (SBS)/montmorillonite (MMT) nanocomposite blends were studied [97]. MMT/SBS nanocomposites were prepared in an internal mixer, by adding an epoxidized SBS (SBSe) as a compatibilizer, and they were then added to PP in concentrations up to 10 wt%. Fig. 12(a–f) report the TEM micrographs of the prepared blends. The unfilled PP/SBS alloy was characterized by the presence of the largest domains, while the introduction of MMT led to a substantial refinement of the morphology, probably due to the increase of the dispersed phase melt viscosity, which hindered the coalescence of rubber droplets. It is also interesting to note that the addition of SBSe did not substantially affect the SBS domains size, but induced the MMT to be preferentially located at the PP/SBS interface. Consequently, the combined use of both MMT and SBSe compatibilizer led to an enhancement of the impact strength by about 60%, with a retention of the elastic modulus.

Chandran et al. investigated the mechanical properties of PP/natural rubber (NR) blends compatibilized with the addition of nanoclay, observing a linear reduction of the dimension of the NR domains up to 3 μm with an NC amount of 5 phr. A further increase in the nanoclay content did not lead to a further decrease of the NR droplets size, meaning that the interfacial saturation was reached at that nanofiller loading [98]. Recently Azizl et al. prepared through melt mixing PP/EVA elastomeric blends compatibilized with *n*-butyl acrylate glycidyl methacrypoles terpolymer (PTW) and nanofilled with graphene and graphene oxide. It was highlighted that the addition of both nanofillers in the presence of PTW led to a

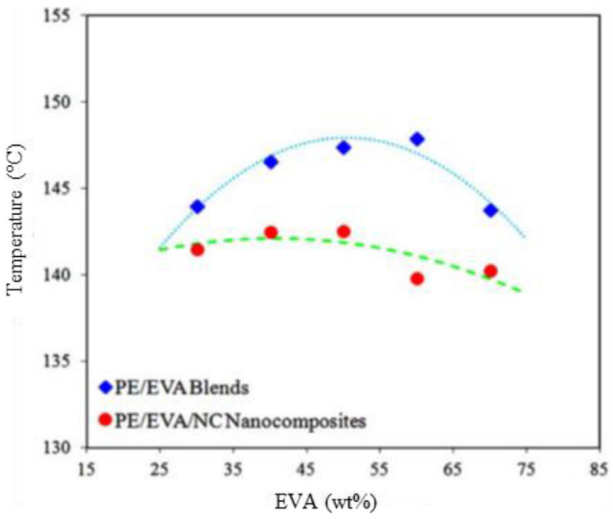

Fig. 11. Phase diagram of PE/EVA blends and PE/EVA/NC nanocomposite blends (reprinted with permission from Ref. [95]).

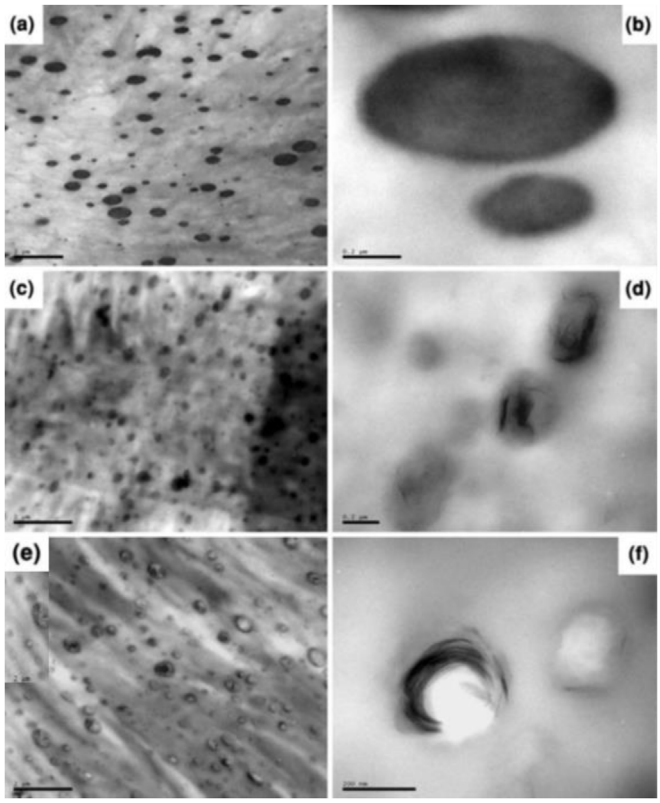

Fig. 12. TEM micrographs of PP/SBS blends (SBS content = 10 wt%). (a,b) Uncompatibilzed blend, (c,d) blend with a MMT content of 0.3 wt%, (e,f) blend with a MMT content of 0.3 wt% and an SBSe amount of 0.5 wt% (reprinted with permission from Ref. [97]).

reduction of the size of EVA dispersed droplets, with a migration of the nanofillers to the PP/EVA interface. Moreover, both creep and recovery compliance of these blends were reduced through the incorporation of PTW and increasing the nanofillers concentration [99]. In a recent paper PP/epichlorohydrin rubber (ECH) based thermoplastic elastomer (TPE) blends were compatibilized with a random ethylene-acrylic ester-maleic anhydride terpolymer (EAMAT) and nanofilled with reduced graphene oxide (rGO) nanosheets [100]. Considering that graphene oxide (GO) is constituted by hydrophilic and easily dispersible planar sheets of covalently bonded carbon atoms containing different oxygen functional groups (e.g. hydroxyl, epoxide, and carbonyl groups), reduced graphene oxide can be generally obtained through chemical (i.e., by using hydrazine or hydrazine derivatives) or thermal (i.e., from 300 to 1000 °C) reduction processes of GO, aiming at restoring the pristine graphene structure [101]. In many cases, rGO can be also functionalized or decorated with metallic nanoparticles and nanostructures, to be utilized in several fields such as catalysis, optics, biochemical sensing, electronics and spectroscopy [102]. In that manuscript SEM micrographs, atomic force microscopy and contact angle measurements evidenced the preferential localization of rGO in the continuous PP phase and at the PP/ECH interface. The improvement of the mechanical, rheological and viscoelastic properties observed in these blends was explained considering that, during the straining process, rGO nanosheets promoted the orientation of the PP macromolecules. In a paper of Evgeni et al. PP/nylon/alumina nanocomposite blends were prepared through batch compounding, by using several types of PP and alumina nanoparticles with different size (from 13 to 500 nm). Under certain processing conditions, the addition of nanoparticles promoted an important compatibilization, significantly affecting both the melt viscosity and the morphological behavior of the nanofilled blends [103]. Paran et al. investigated the mechanical properties of PP/poly(trimethylene terephthalate) (PTT)/clay nanocomposites, by using two kinds of organomodified clays and two compatibilizers having different chemical affinity to the polymer components. X-ray diffraction, TEM microscopy and tensile tests revealed that, depending on the chemical nature of the compatibilizer and on the clay loading, the nanofiller was localized either in the PTT phase or at the PP/PPT interfacial region, with an increase of both the elastic modulus and of the tensile strength with the nanoclay amount [104]. Feng et al. reported that nanosilica in PP/PS blends was located at the interface, and that this nanofiller was able to substantially suppress the coarsening of the morphology [105]. Also Wang et al. found a similar effect in PP/PS alloys by adding small amounts of organoclay (2–5 wt%) [106].

Zhang et al. investigated the non-specific compatibilizing action of different large aspect ratio nanofillers, ranging from nanotubes to nanoclays, in a model PS/PMMA blend. It was concluded that in these alloys the compatibilization was related to the presence of fillers, able to form in situ grafts with the immiscible components. Moreover, through theoretical studies, it was found that the compatibilization process was strongly influenced by the aspect ratio and by the bending energy of the nanofillers [89]. Thompson et al. studied the influence of the extensional strain and of the strain rate on the morphology of nanofilled PS/high density polyethylene (HDPE), processed through different converging dies attached to the outlet of a capillary viscometer. It was found that the extensional flow was very effective in reducing the size of the dispersed HDPE droplets and that the addition of fumed silica at a concentration of 4 wt% promoted a further refinement of the morphology, even if the final result was only slightly better than that observed with the help of the extensional flow alone [107]. The paper of Istrate et al. was focused on the morphological and mechanical investigation of nanoclay filled PS/PP blends (relative ratio = 70/30 wt%), prepared with or without maleated PP, utilized as compatibilizer. In non-compatibilized PS/PP/clay blends the nanofiller was localized only in the PS component, whereas in compatibilized systems nanoclay was dispersed in both phases. Regardless of the position of the nanofiller within the blends, it was shown that the addition of clay significantly decreased the dispersed PP domain size and modified the crystallinity degree, improving the stiffness of the material [108].

Electrically conductive PA6/ABS nanocomposite blends, compatibilized with maleic anhydride-grafted acrylonitrile-butadiene-styrene (ABS-MA), were prepared by Luna et al. through melt compounding and injection molding, by adding functionalized MWCNTs [109]. The homogeneous dispersion of MWCNTs within the blend obtained at a filler amount of 1 phr was responsible of its antistatic properties and of the noticeable increase of the impact strength (221%) with respect to the neat PA6. Moreover, the presence of MWCNTs accelerated the crystallization and increased the heat deflection temperature (HDT) by 20 °C compared to the PA6 matrix. These beneficial effects could be correlated to the microstructural features of the nanofilled blends. Fig. 13(a–c) highlight that these nanocomposites showed the typical ductile fracture morphology, characterized by a rough surface and an evident plastic deformation. Moreover, increasing the MWCNTs amount, a refining of the dispersed ABS domains could be observed. This effect was explained considering that the selective nanofiller dispersion in the PA6 phase changed its rheological behavior, influencing the deformation and the

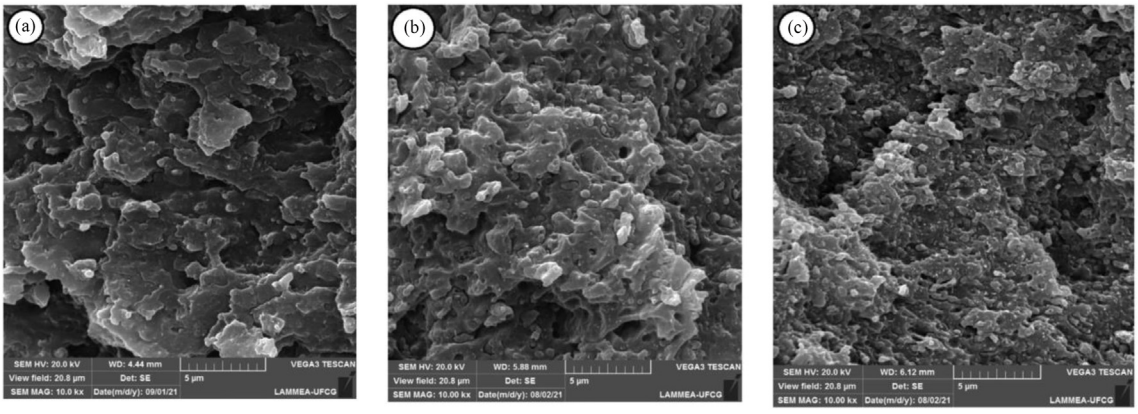

Fig. 13. SEM micrographs of PA6/ABS/ABS-MA/MWCNTs nanocomposite blends. MWCNTs loading of (a) 1 phr, (b) 3 phr, (c) 5 phr (reprinted with permission from Ref. [109]).

breakdown of the dispersed phase, lowering thus the size of the ABS droplets.

Cao et al. investigated the compatibilizing effect of graphene oxide (GO) in an immiscible polyamide (PA)/polyphenylene oxide (PPO) alloy, showing that with a GO content of 0.5 wt% the size of the dispersed PPO phase was dramatically reduced. In this work, the compatibility improvement observed in nanofilled blends was ascribed to the strong interaction of GO with both PA and PPO phases, which led to a reduction of their interfacial tension [110]. In the case of PA6 based blends, it is also interesting to highlight the possibility to insert reactive nanofillers. For instance, in a paper of Guo et al. an in situ compatibilization of PA6/PC blends through interfacial localization of reactive silica nanoparticles was proposed [111]. A methacrylic monomer was grafted onto the silica surface and then copolymerized with styrene and 3-isopropenyl-α,α′-dimethylbenzyl isocyanate (TMI). When PA6 and PC were melt blended at a relative concentration 70/30 wt% with the surface modified SiO_2 (SiO_2-PST), PA6 chains were grafted onto the SiO_2-PST nanoparticles to form PA6-SiO_2-PST through a reaction between the terminal amine groups of the PA6 and the isocyanate moieties of the PST grafts. With an optimum TMI concentration, SiO_2-PST nanoparticles were preferentially located at the PA6/PC interface, with a significant decrease in the PC droplets size from 1.6 μm to 0.6 μm. The addition of SiO_2-PST nanofiller at a concentration of 0.5 wt% increased the tensile strength from 64 to 80 MPa, the elongation at break from 85 to 285%, and the Charpy impact strength from 10.3 to 29.4 kJ/m^2.

Yousfi et al. prepared by melt extrusion nanofilled PET/PE alloys (relative ratio = 80/20 wt%), by adding two commercial organomodified nanoclays (i.e., Cloisite® 10A and 30B) and another montmorillonite surface modified at lab scale with a thermally stable phosphonium surfactant through a cationic exchange reaction [112,113]. It was found that the size of the dispersed PE droplets and the ductility of the blends was affected by the thermal stability of the clay organomodifier rather than by the enthalpic interactions between the blend components and the nanoclay surfactant. Therefore, the best mechanical performances and compatibilization efficiency were detected in the case of phosphonium organomodified clay nanocomposite blends. A similar conclusion could be drawn also considering the properties of PET/PE alloys containing the surfactants alone without clay, demonstrating thus the efficacy of the phosphonium organic modifier as a compatibilizer.

Nowadays, PC/ABS blends are one of the most used plastic alloys in the industry, as they find wide application mainly in the electronic and automotive sectors. In literature it was demonstrated that the addition of graphite nanoplates (GnP) [114–116] and graphene oxide (GO) [117] in PC/ABS blends (relative ratio = 85/15 wt%) could noticeably enhance their thermo-mechanical and flammability properties. In a recent study by Anjos et al. the effect of the addition of GnP and maleic anhydride grafted ABS (ABS-MA) on the rheological, thermo-mechanical and electromagnetic properties of PC/ABS alloys was investigated [118]. Mechanical tests showed that ABS-MA acted as an efficient blend compatibilizer, while GnP introduction significantly increased the thermal stability, the Shore D hardness and the tensile properties at all the relative compositions. Moreover, it was observed that GnP and ABS-MA had a synergistic effect on the mechanical performances of these blends, with a doubling of the strain at break at a GnP loading of 3 wt%. Furthermore, a slight increase of the electromagnetic waves attenuation (up to 2 dB) was detected for this composition. Sinha Ray et al. studied the compatibilization efficiency of organoclay in a PC/PMMA blend, showing that with a nanoclay loading of 6 wt% it was possible to obtain a significant decrease of the size of the dispersed PC domains [119]. Also Taraghi et al. highlighted a reduction in the size of the dispersed ethylene-propylene copolymer (EPC) droplets in PC/EPC alloys upon the introduction of MWCNTs at a concentration of 1.5 wt% [120].

Besides nanocomposite blends constituted by the most common engineering thermoplastics, in literature there are many other examples of thermoplastic polymer alloys in which different kinds of nanofiller were added.

For instance, the influence of untreated (U1) and stearic acid surface treated (U1S2) calcium carbonate ($CaCO_3$) nanoparticles on the performances of polyurethane (PU)/poly(vinyl acetate) (PVAC) alloys was investigated [121]. Thanks to the determination of the adhesion parameters and wetting factor of PU, PVAC, U1, and U1S2, it was highlighted that U1 was preferentially localized in the PU component, while U1S2 was located at the PU/PVAC interface. U1S2 nanofilled blends were characterized by lower tensile strength and elongation at break with respect to the corresponding U1 filled alloys, because of the different surface properties of these nanoparticles. It was therefore concluded that the mechanical features of nanofilled polymer alloys are influenced by the overall blend morphology, and not only by the nanofiller localization.

In another paper, GnPs were introduced into poly(vinylidene fluoride) (PVDF)/poly(ethylene oxide) (PEO) blends through solution casting [122]. It was evidenced that GnPs were preferentially located in the PVDF phase and/or at the PVDF/PEO interface, and the determination of the wetting parameter for this nanocomposite alloy confirmed a better affinity of GnPs with the PVDF component. The compatibilization efficiency provided by GnPs on these blends was established through a rheological method, and an enhancement of both binodal (T_b) and spinodal (T_s) decomposition temperatures was detected upon the introduction of a very limited GnPs amount (0.5 wt%). In a recent work of Torabi et al. electroactive β-phase content of poly(vinylidene fluoride-hexafluoropropylene) (PHP) was increased upon melt blending with PC (at concentrations 10 and 30 wt%) and introducing barium titanate (BT) and/or MWCNTs nanofillers, with the aim to improve the dielectric performances of PHP [123]. SEM results indicated that the best refinement in morphology was obtained with a PC content of 10 wt% and the simultaneous presence of 1.5 wt% of BT and 1.5 wt% of MWCNTs. TEM micrographs highlighted the selective localization of BT in the PHP phase and of MWCNTs in the PC component, while small amounts of both nanofillers were also detected at the interphase. FT-IR, X-ray diffraction analysis and DSC tests evidenced the nucleating effect played by BT and MWCNTs on this blend, with an increase of the β/α ratio, due to the selective localization of these nanofillers.

3.2. Elastomeric based polymer blends

Nowadays elastomers are widely applied in specialty applications like nuclear technology, aerospace, underwater and other defense areas. In the last two decades, several literature works highlighted the increase in mechanical, thermal and barrier properties of elastomers due to the addition of different kinds of nanostructured materials. The addition of nanofillers could be also a promising approach to compatibilize elastomeric based polymer blends, and in literature some papers on this topic can be found.

Natural rubber (NR) is a natural polymer and it is endowed with elevated tensile strength, good flexibility, low compression set, and good tear and abrasion resistance. For this reason, it is widely utilized in industrial products manufactured in part or entirely from NR. Moreover, NR can be used to improve the functional properties of EVA foams. Lopattananon et al. prepared 60/40 wt% EVA/NR blends foamed with azodicarbonamide and nanofilled with sodium montmorillonite and an organoclay [124]. It was found that the selected nanofillers acted as blend compatibilizers, and that sodium montmorillonite was more effective in the development of a better

blend morphology and foam structure. Rubber blends with a nanofiller amount of 5 phr showed superior specific tensile strength with respect to the unfilled alloy, even if the elastic recovery and the compressive strength decreased with the filler loading. Moreover, thermal conductivity measurement showed that nanofiller introduction had a beneficial effect on the thermal insulation properties of these foams.

EPDM, due to its fully saturated backbone structure and the presence of hydrogen bonds in its macromolecular structure, is the elastomer with the highest resistance to radiation. Moreover, it is also characterized by elevated resistance to heat, ozone, cold temperature and moisture. Though the radiation resistance of EPDM is superior to that of the other elastomers, it has a limited solvent resistance, which is a key requirement for nuclear fuel reprocessing facilities. This limitation can be overcome without impairing the radiation resistance upon blending EPDM with other elastomers, like Nitrile Rubber (NBR). In fact, NBR is a special purpose rubber endowed with outstanding oil, fuel and solvent resistance, and it also has elevated thermal stability and low permeability. However, NBR has inferior radiation resistance than EPDM. Following this approach, Ashok et al. prepared by melt compounding and subsequent vulcanization at 170 °C EPDM/NBR blends, compatibilized with maleic anhydride and nanofilled with different amounts (up to 8 phr) of an organomodified nanoclay [125]. X-ray diffraction and atomic force microscopy highlighted the intercalation and exfoliation of nanoclay at lower filler concentrations. Due to the large surface area of this nanofiller and the strong filler/matrix interaction, nanoclay played a compatibilization effect on this blend, as the mechanical and barrier properties (i.e., diffusion, sorption and permeation coefficients) increased with the filler loading. However, at higher nanoclay amounts both mechanical and barrier properties were slightly decreased, due to the formation of nanofiller agglomerates.

Eslami et al. analyzed the effect of nanosilica on the morphological and mechanical properties of EPDM/chloroprene rubber (CR) nanocomposite blends [126]. TEM and SEM micrographs revealed that nanoSiO_2 was present in both EPDM and CR components, while the analysis of the glass transition temperature values (T_g) showed that the EPDM/CR compatibility was enhanced with the introduction of nanosilica. The compatibilizing action of this nanofiller, together with its reinforcing capability, led to a general improvement of the thermo-mechanical properties of these compounds. In particular, the tensile strength, elongation at break and modulus of the 50/50 phr blend nanofilled with 10 phr of nanosilica (CR50/S) were enhanced by around 398%, 33%, and 135%, respectively (see Table 1). Also the dynamic behavior was strongly affected by nanosilica introduction, as the storage modulus above the glass transition temperature of the 50/50 phr alloy (CR50) was increased from 3.9 to 7.2 MPa upon a SiO_2 addition of 10 phr.

3.3. Blends with thermosetting polymers

Due to the largely unfavorable enthalpy of mixing, the greatest part of thermoplastic (TP)/thermosetting (TS) alloys is immiscible, and thus characterized by a phase-separated morphology and by limited thermo-mechanical properties. However, when the TS component is the continuous phase of the blend, a noticeable increase in the stress at break, the fracture toughness and the stress at break can be often obtained. Therefore, in many cases the objective is to have a continuous TS phase, keeping the TP as the major component [58]. In this sense, nanofillers addition could induce a better compatibility, leading thus to better physical properties of the resulting blends. In literature only few papers dealing with TP/TS nanocomposite alloys can be found, and in the greatest cases the thermoplastic polymer was mixed with an epoxy resin.

Table 1
Mechanical properties of EPDM/CR blends and their relative nanocomposites (adapted from Ref. [126]).

Sample	Tensile modulus (MPa)	Tensile strength (MPa)	Elongation at break (%)	Shore A
CR0	3.1 ± 0.1	1.9 ± 0.1	253 ± 6	56
CR50	2.6 ± 0.2	2.5 ± 0.5	596 ± 65	61
CR100	2.6 ± 0.3	2.6 ± 0.2	636 ± 14	75
CR0/S	4.5 ± 0.1	7.5 ± 0.4	754 ± 20	67
CR50/S	6.2 ± 0.1	12.3 ± 0.2	794 ± 7	75
CR100/S	5.4 ± 0.5	15.0 ± 1.0	871 ± 25	82

Li et al. analyzed the crystallization behavior of PP/epoxy resin blends filled with CB nanoparticles and compatibilized with PP-g-MAH [127]. The analysis of the non-isothermal crystallization parameters revealed that both CB and the dispersed epoxy particles acted as nucleating agents, accelerating the crystallization process in the continuous PP phase. The introduction of CB nanoparticles, preferentially localized in the epoxy component, changed the shape of the spherical epoxy domains into elongated structures, reducing thus the nucleating effect played by the epoxy phase. Moreover, the introduction of PP-g-MAH produced a substantial morphology refinement, decreasing the size of the epoxy particles and further promoting PP crystallization.

Diez-Pasqual et al. prepared epoxy/ethylene/1-octene copolymer blends nanofilled with MWCNTs, with the aim to increase the toughness of the TS phase [128]. Both the dispersed thermoplastic phase and MWCNTs affected the curing process of the epoxy, accelerating the curing onset but slowing its progress. Nanocomposites with limited MWCNTs amounts were characterized by a droplet-like morphology, in which TP domains were dispersed within the continuous epoxy component, and the nanofiller was localized near the TS/TP interphase (see Fig. 14). This peculiar morphology led to improved thermal stability and a good balance between stiffness, strength and toughness.

Salehi et al. investigated the role of an organoclay on the microstructural and rheological properties of PBT/epoxy nanocomposite blends, with particular attention of the effect played by the feeding order and by the curing process of the epoxy [129]. Nanocomposite polymer alloys were prepared through melt compounding at 240 °C, according to three feeding routes, i.e., (i) simultaneous feeding, (ii) PBT/organoclay based masterbatch feeding, (iii) epoxy/organoclay based masterbatch feeding. Regardless of the feeding order, all the prepared blends were characterized by a highly intercalated microstructure. Linear viscoelastic tests on uncured samples, prepared according to feeding routes (i) and (ii), revealed a pronounced low frequency non-terminal behavior, whose extent increased in the cured blends. It was thus concluded that the majority of the organoclay was localized in the PBT component. Interestingly, alloys prepared following the feeding order (iii) did not evidence an appreciable low frequency solid body response, meaning that nanoclay migration from the epoxy domains to PBT matrix was the time consuming process, because of the elevated nanoclay aspect ratio and the high viscosity of the PBT phase. Moreover, in this work it was concluded that the curing process did not substantially affect the extent of nanoclay intercalation and/or dispersion, but it could increase PBT/epoxy interfacial interaction.

Vyas et al. developed PA6/nanoclay nanocomposites through in-situ polymerization, and then blended the resulting materials with an epoxy resin through reactive blending [130]. A noticeable enhancement of PA6 crystallinity degree and of the viscosity of PA6/epoxy blend were detected upon a nanofiller addition of 0.5 wt %, while the opposite trend was observed increasing the nanoclay loading (up to 10 wt%). The crystallinity increase detected at low

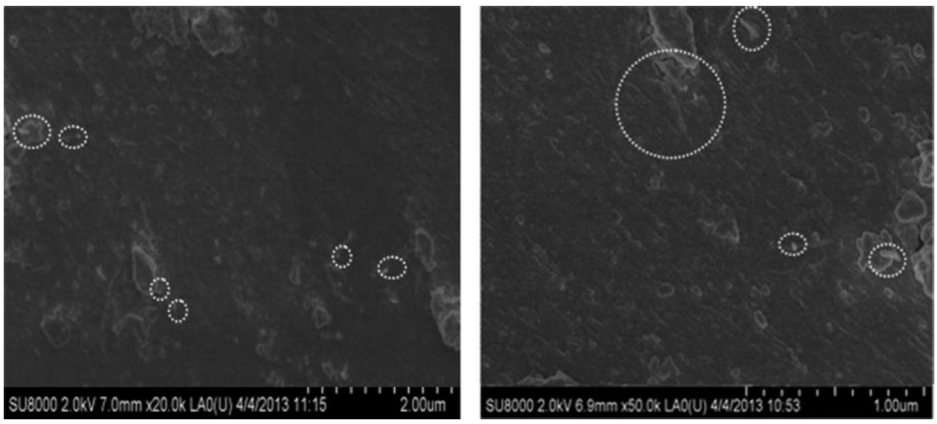

Fig. 14. SEM micrographs at different magnifications of TS/TP/MWCNTs nanocomposite blends (TP content = 5 wt%, MWCNTs amount = 5 wt%). The dashed circles show MWCNTs located close to the TP particles (reprinted with permission from Ref. [128]).

nanoclay concentration was explained considering that, during curing, nylon 6 generally crystallized in form of spherulites along with branching and growing radially outward to occupy the free volume by using epoxy surface as heterogeneous phase. In the present work, PA6 was first nanomodified with nanoclay during polymerization, and the crystallization took place before blending with epoxy, because of the formation of hydrogen bonds between PA6 macromolecules and hydroxyl groups present on the surface of the nanoclay. It was thus concluded that PA6 preferably crystallized over clay lamellae instead around epoxy particles.

4. Effect of nanofiller addition in bioplastic based polymer blends

A possible solution to the environmental concerns on the pollution generated by fossil fuel based polymers and on the problems related to the management of plastic waste could be represented by bioplastics, i.e., polymers that are biodegradable and/or derived from renewable resources. Biodegradable plastics can limit the amount of plastic waste produced, while bioderived polymers can lead to a noticeable carbon footprint reduction in the first stage of the life cycle of plastics, i.e., in the extraction of resources [1]. In the last two decades, different kinds of bioplastics have reached the commercialization phase, i.e., poly(lactic acid) [131], thermoplastic starch (TPS) [132], poly(butylene succinate) (PBS) [133], polyhydroxyalkanoates (PHAs) [134], but also the renewable counterparts of some fossil fuel based polymers, like bio-polyethylene (bioPE) and bio-poly(ethylene terephthalate) (bioPET) [135]. However, nowadays the extensive industrialization of bioplastics is still in its embryonic stage, as the worldwide bioplastic production in 2019 was 2.11 MT, i.e., only 0.6% of the global plastics production, and it is forecasted to reach 2.89 MT by 2025 [1]. The rapid expansion of the bioplastics market is limited by their more expensive production and by their lower thermo-mechanical properties with respect to traditional polymers. However, considering the ever-increasing demand of suitable alternatives to fossil fuel based polymers, a considerable increase of the bioplastics market could be expected in the next years.

The increasing interest in bioplastic based polymer blends can be motivated by the need of developing novel sustainable materials with better properties and processability, and with a lower cost. Also the formulation of blends constituted by biodegradable and non-biodegradable matrices represents an interesting possibly towards the production environmentally friendly plastics, as they are characterized by a higher degradation rate with respect to fully non-biodegradable blends [136]. In the book of Utracki it is possible to find many examples of commercial bioplastics based blends [3]. Since almost all bioplastics based blends are immiscible and present a relatively poor interfacial interaction, the need for bio-based compatibilizers and/or of novel compatibilization strategies is of utmost importance. Among all the compatibilization techniques, particularly interesting is the nanofiller induced compatibilization, in which the addition of solid nanostructured materials can limit the phase separation, refining the blend morphology and also improving the interfacial adhesion. It is important to underline that a proper nanofiller selection can also strongly improve the other physical and mechanical properties [137]. In this Chapter, an overview of some representative examples of nanocomposite blends with bioplastics is reported, with particular attention to the role played by the nanofiller on the compatibilization of these alloys.

The greatest part of the papers in literature on nanocomposite blends based on bioplastics is referred to poly(lactic acid). PLA is an aliphatic polyester that is usually synthesized by ring-opening polymerization of lactide, obtained by fermentation of starch-rich plants (i.e., rice, corn, cassava, sugarcane). PLA is characterized by a good balance of properties (mechanical, thermal, biodegradation, transparency, barrier) and processability, and it is thus widely applied in agriculture, packaging, textile, and automotive industries [138]. However, the brittleness and the limited barrier properties of PLA have hindered its industrial and commercial expansion [1]. The addition of nanofillers and the blending with other polymers can represent valuable strategies to overcome some of the PLA shortcomings. Therefore, PLA has been recently mixed with polyethylene glycol, ethylene vinyl alcohol, poly(butylene adipate-co-terephthalate), and other bioplastics to enhance its crystallinity and its thermo-mechanical performances. Fredi et al. tried to improve the toughness of PLA solvent-cast films upon blending with 10 wt% of poly(decamethylene 2,5-furandicarboxylate) (PDeF), and by adding rGO nanofiller at different amounts [137]. In Fig. 15(a–e) SEM micrographs of the cryofracture surface of the PLA-PDeF10 and PLA-PDeF10-rGOx (x = 0.25–2 phr) blends are reported. From Fig. 15(a) it is evident that the unfilled blend (PLA-PDeF10) was immiscible, and the microstructure was characterized by PDeF smooth spheroidal domains with a poor interfacial interaction with PLA, having a mean diameter of 1.9 μm. Nanofiller addition considerably modified the morphology and improved the compatibility of the blend, as the introduction of 0.25 phr of rGO decreased the diameter of the dispersed PDeF droplets up to 1.4 μm, enhancing their roughness and their interfacial interaction with the PLA phase

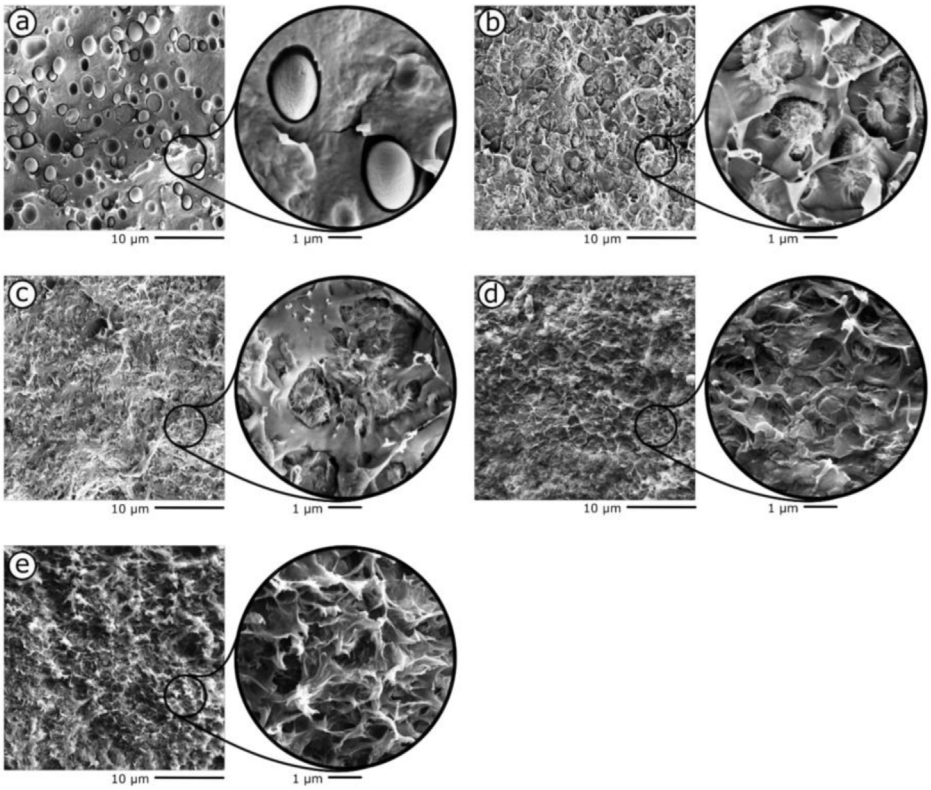

Fig. 15. SEM micrographs of the cryofracture surface of (a) PLA-PDeF10, (b) PLA-PDeF10-rGO0.25, (c) PLA-PDeF10-rGO0.5, (d) PLA-PDeF10-rGO1, (e) PLA-PDeF10-rGO2 films (reprinted with permission from Ref. [137]).

(Fig. 15(b)). An increase in the rGO loading produced further morphological changes, with the disappearance of PDeF droplets at the highest nanofiller concentrations (Fig. 15(c–e)). Moreover, from these micrographs, it can be seen that rGO was preferentially localized in the PDeF phase until a nanofiller amount of 0.5 phr, while it was also present in the PLA component at higher filler contents. DSC tests confirmed the immiscibility of the produced blends at all the investigated compositions, and showed that rGO addition led to a crystallinity enhancement in both polymer phases. TGA measurements highlighted the positive impact of rGO and PDeF on the thermal degradation resistance of PLA. The compatibilizing effect played by rGO on these blends was highlighted also by tensile tests, as the elongation at break of PLA was considerably enhanced by adding 10 wt% of PDeF and a limited rGO concentration (0.25 phr), passing from 5% up to 76%. A further increase of the rGO amount produced a toughness decrease due to nanofiller agglomeration, but both the stiffness and the strength were enhanced up to an rGO content of 1 phr.

Bher et al. prepared PLA/thermoplastic starch (TPS) nanocomposite blends, performing a compatibilization upon the introduction of maleic anhydride and of a peroxide radical during the reactive blending extrusion process, and by adding commercial graphene nanoplatelets [139]. The addition of this nanofiller was responsible of a noticeable increase of the elongation at break and of the fracture toughness (900% compared to neat PLA, 500% with respect to the unfilled blend), due to the crack bridging effect promoted by the high aspect ratio of the nanoplatelets. Moreover, nanofilled blend showed a 50% reduction of the oxygen permeability coefficient with respect to neat PLA.

Pristine boehmite nanorods (p-BNRs) and epoxidized boehmite nanorods (m-BNRs) have been synthesized and incorporated in PLA/PBS blends by Li et al. [140]. Both p-BNRs and m-BNRs were preferentially located at the interface, and the two nanocomposites presented very similar morphologies. However, their mechanical behavior was completely different. Compared with the unfilled PLA/PBS blends, nanocomposites with m-BNRs showed increased elongation at break, impact strength and yield strength, while p-BNRs filled nanocomposites were characterized by a general deterioration of the mechanical properties. This discrepancy was explained considering that p-BNRs at the interface had barren surface and did not interact with the surrounding polymer phases, while the epoxide groups on m-BNRs reacted with the carboxylic acid groups of both polymer components, generating thus polymer chains chemically bonded to the nanorods at the interface and thus enhancing the PLA/PBS interfacial adhesion (see Fig. 16).

Thiyagu et al. prepared biodegradable PLA/PBAT blends through film casting at a fixed relative ratio (90/10 wt%), adding also 5 wt% of a cardanol oil (CO) compatibilizing agent and 1 wt% of different nanoparticles (ZnO, TiO_2, and SiO_2). It was shown that the introduction of both CO and the nanoparticles determined an improvement of the tensile strength and of the strain at break, an enhancement of the barrier properties, better optical properties and surface hydrophobicity [141]. Bitinis et al. developed PLA/NR/organoclay nanocomposite blends, evidencing that nanoclay was preferentially located at the interface and acted as a compatibilizer between the polymer phases [142].

In the paper of Wu et al. zirconium phosphate (ZrP) nanoparticles and EGMA copolymer were added into PLA upon reactive melt blending, in order to improve its toughness [143]. It was reported that the impact strength of PLA/EGMA/ZrP (82/15/3 wt%) nanocomposite was increased of about 22 times with respect to neat PLA. FT-IR analysis highlighted that some compatibilization reactions between the components took place during the reactive blending process. SEM micrographs of the fracture surface showed

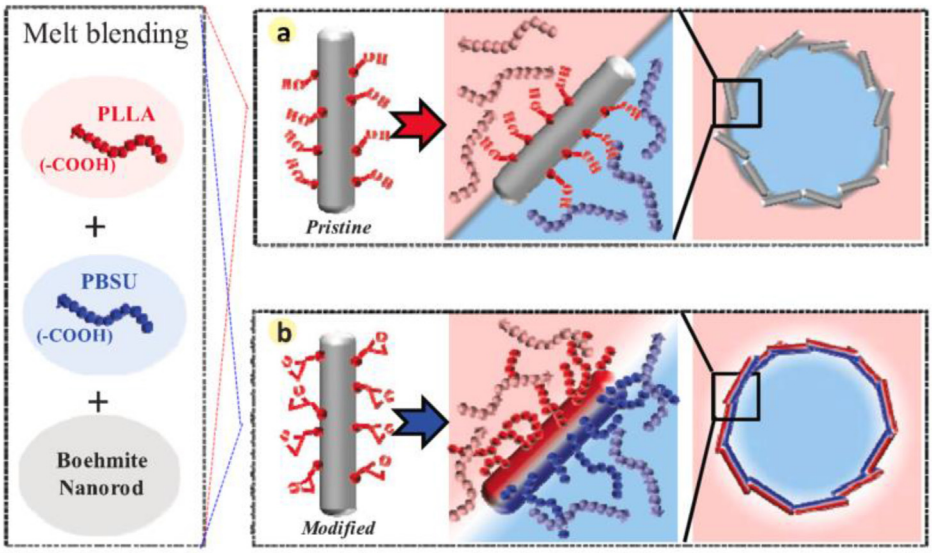

Fig. 16. Schematic diagram of p-BNRs and m-BNRs filled PLA/PBS nanocomposite blends (reprinted with permission from Ref. [140]).

the formation of a typical core-shell morphology, with ZrP nanoparticles wrapped by the EGMA phase, responsible for the elevated plastic deformation observed in the nanofilled blend. This noticeable toughness increase was related to the effective interfacial compatibilization and massive shear yielding deformation obtained through the synergy of EGMA with ZrP in the PLA phase.

De Oliveria et al. investigated the rheological and morphological properties of PLA/bioPE blends compatibilized with maleic anhydride grafted polyethylene (MA) and filled with calcium carbonate nanoparticles [136]. SEM micrographs showed that $CaCO_3$ introduction affected the dispersion of PLA domains in the bioPE matrix, leading to the formation of a co-continuous morphology. Rheological characterization confirmed the morphological evidences, as the addition of $CaCO_3$ improved the solid-like behavior of the blend. It was hypothesized that the nanofiller could act as a co-compatibilizer in these alloys, as most $CaCO_3$ particles migrated to the phase boundary, where also the compatibilizer was present. The coexistence of the MA compatibilizer and of $CaCO_3$ nanofiller in the interfacial region altered the stress gradient, giving more freedom to previously restricted PLA macromolecules. In these conditions, the thickness of the boundary region was increased and physical interactions could occur between the macromolecules, resulting in a network like morphology responsible for the increased elasticity of the material (see Fig. 17).

Immiscible PBS/HDPE nanocomposite blends were prepared by Darshan et al. through melt mixing process, by adding maleated PE (MA) as compatibilizer and CNTs as reinforcing nanofiller [144]. SEM micrographs revealed that MA played an efficient compatibilizing action, decreasing the size of the dispersed HDPE droplets, while CNTs were preferentially distributed in the HDPE phase, leading to the formation of a pseudo-double percolated structure, as also confirmed by rheological tests. DSC tests highlighted the nucleation effect played by CNTs on the crystallization of the HDPE phase, while MA accelerated the crystallization of PBS. Interestingly, the stiffness of the blend with a CNTs content of 3 phr was increased up to 50% with respect to neat PBS, while its electrical resistivity was dramatically reduced (up to 8 orders of magnitude).

5. Effect of nanofiller addition in recycled polymer blends

Generally speaking, there are three main methods of plastic waste recycling: mechanical recycling, feedstock recycling, and energy recovery. The most desirable is the former, hence this Chapter will focus on mechanical recycling technology. The first step of the mechanical reprocessing of plastic waste is the sorting of mixed polymers. Sorting process could be expensive, but it can lead to high performance recyclates, while the recycling of unsorted polymers, even if cheaper, generally leads to products with unsatisfactory properties. In this sense, polymer blending could be an effective option for future recycling technology, as it could partially solve the technical limitations related to the need of sorting mixed plastics waste, with or without the introduction of compatibilizers

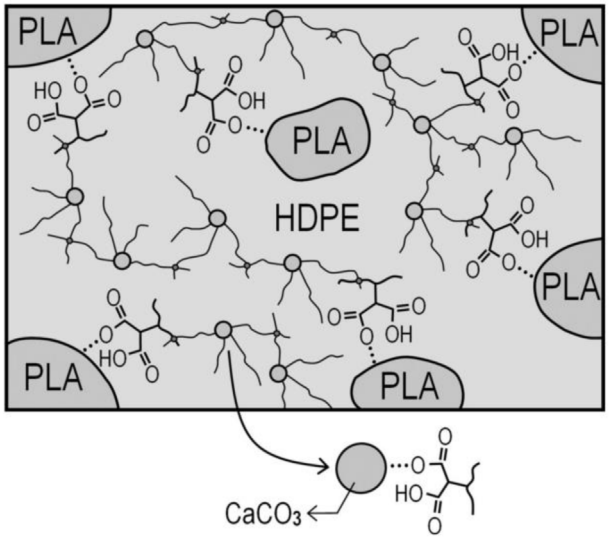

Fig. 17. Illustration of the co-interaction proposed for $CaCO_3$ and MA in PLA/bioPE nanocomposite blend (reprinted with permission from Ref. [136]).

[145,146]. In fact, polymer blends often present good processability and versatility, and recycled blends can be also upgraded upon the addition of suitable chemicals and/or additives [147]. The upgrading process can also overcome the problems related to the fact that the starting blend could be degraded (i.e. photoxidized, partially biodegraded, thermally degraded, etc.). Particular attention should be put on the presence in the blends of other components, like fillers, that can affect the thermal degradation behavior during the reprocessing [148], especially when biodegradable polymers must be recycled [149,150]. In the mechanical reprocessing of polymer alloys it is of utmost importance the regeneration of the pristine microstructure, in order to obtain alloys with stable and reproducible performances. This could be accomplished through the adoption of suitable processing parameters and through the re-compatibilization of the blend. In this sense, re-compatibilization of polymer mixtures is able to restore the morphology and to improve the interfacial adhesion between the different phases. Also the addition of both micro- and nanostructured fillers has been recently applied as an interesting re-compatibilization technique, able to recover the original performances of the blend and/or to impart peculiar properties. In particular, the addition of nanoparticles to recycled mixed plastics can improve their processability and their performances, it can reduce operational costs, and it can also provide a strong compatibilizing action [151]. Therefore, an analysis of the role played by nanofillers introduction on the recyclability of polymer blends and on the properties of the resulting recyclates will be reported in this Chapter.

Arman et al. analyzed the individual effect of MWCNTs and nanoclay on the properties of uncompatibilized blends constituted by recycled HDPE and recycled PET [152]. The alloys were prepared through twin screw extrusion followed by compression molding, fixing an HDPE/PET ratio of 75/25 wt% and by adding different nanofiller amounts (from 0.5 to 6.0 phr). Polymer granules and the MWCNTs were manually mized and then melt-blended in a co-rotating screw extruder operating at 30 rpm, adopting a temperature profile of 250, 270, 240, and 190 °C (from feeder to die). The extruded material was then granulated and compression moulded for 10 min in a hot press at 200 °C under a pressure a 1000 psi. It was shown that MWCNTs nanocomposites with a nanofiller loading of 4 phr showed the optimum tensile strength (14.5 MPa), elastic modulus (587 MPa), and strain at break (4.2%), while for clay nanocomposites the best mechanical performances were obtained with a filler concentration of 1 phr (see Fig. 18). However, the impact strength was reduced upon the addition of both nanofillers.

Recycled HDPE/PET/organoclay nanocomposites have been also developed by Chen et al. via melt intercalation, and their microstructural and mechanical behavior was analyzed [153]. Recycled PET pellets and organoclay were preliminary dried at 100 °C for 24 h, and melt mixing of was then performed in a laboratory scale co-rotating twin screw extruder. The nanocomposites were prepared using either a one-step or a two-step compounding, fixing a HDPE/PET ratio at 75/25 wt%. In the one-step method, all of the raw materials (i.e., HPDE, PET, 5 phr of ethylene-glycidyl methacylate compatibilizer) were added simultaneously and compounded at a screw speed of 30 rpm and a barrel temperature profile of 190–240–270–250 °C (from feeding to die zones). In the two-step blending method, a masterbatch was first made by melt-blending both of recycled polymer matrix components with 5 phr of ethylene-glycidyl methacylate. In first extrusion, a temperature profile of 190–240–270–250 °C and a screw speed of 30 rpm were used. In the second step of extrusion, the masterbatch was blended with organoclay at a screw speed of 30 rpm and a temperature profile 170–215–210–195 °C. The extrudates were then granulated into pellets and compression moulded at 200 °C under a pressure of 1000 psi for 15 min. It was shown that the best compatibility

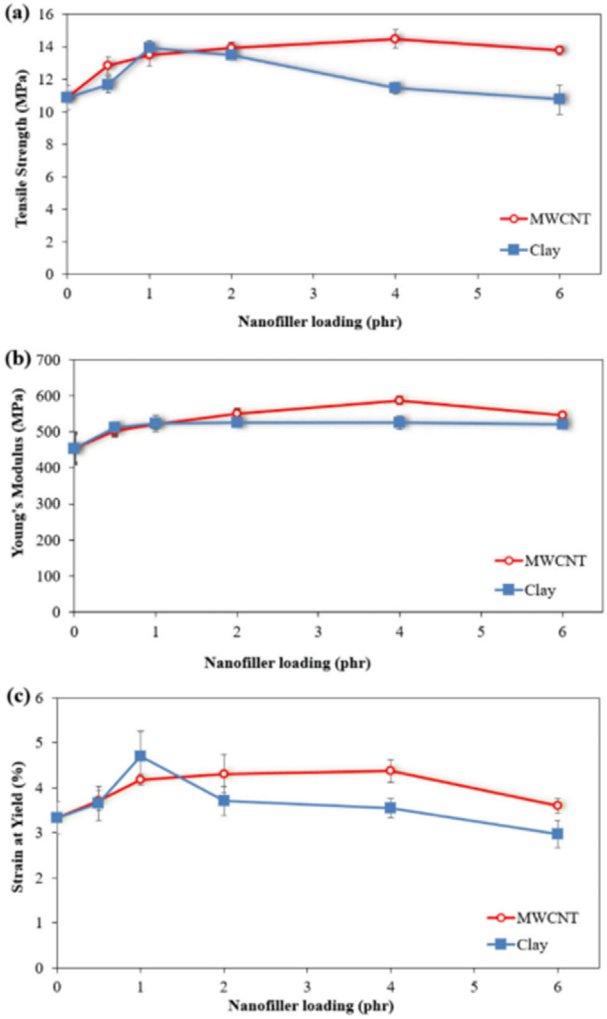

Fig. 18. Effect of MWCNTs and nanoclay loading on (a) tensile strength, (b) Young's modulus, and (c) strain at yield of recycled HDPE/PET nanocomposite blends (reprinted with permission from Ref. [152]).

between HDPE, PET and organoclay, the higher degree of nanoclay exfoliation and the best mechanical properties were obtained upon the simultaneous introduction of nanoclay and an ethylene-glycidyl methacylate compatibilizer into the recycled HDPE/PET alloy. Even if the stiffness of the nanocomposite increased with the nanoclay amount, the tensile strength, the impact strength and the elongation at break were negatively affected by the nanofiller introduction, especially at elevated concentrations, because of the formation of clay agglomerates. A similar approach was also proposed by the same authors [154,155], introducing rice husk flour (RHF) at different loadings (from 40 up to 80 wt%) in recycled HDPE/PET blends. Recycled HDPE and PET were melt blended using a laboratory scale co-rotating twin screw extruder, operating at 30 rpm and setting a barrel temperature profile of 250–270–240–190 °C (from the feeding to die zone). Blends were prepared at a fixed HDPE/PET ratio of 75/25 wt% and by adding 5 phr of an ethylene-glycidyl methacylate compatibilizer. Pre-extruded pellets were then compounded with RHF (previously dried in an oven at 90 °C for 24 h) and 3 phr of a maleic anhydride grafted polyethylene (MA), setting a temperature profile 170–215–210–195 °C, with the same screw speed. After extrusion, the resulting materials were compression moulded at 200 °C under a pressure of 1000 psi for 15 min. It was noticed that, regardless to

the RHF addition, the presence of the compatibilizer improved the tensile properties (i.e., elastic modulus and stress at break) of the resulting blends, thanks to a better HDPE/PET interfacial adhesion.

Marotta et al. introduced small concentrations of an organo-modified clay (Cloisite® 15A) in a ternary alloy constituted by HDPE, PP, and PET coming from mixed color flaxes from household waste [156]. Nanofilled blends were prepared using a co-rotating twin screw extruder, fixing a relative HDPE/PP/PET ratio of 37.5/37.5/25 wt% and by adding 2 phr of organoclay. Extrusion was performed setting a temperature profile 210–230–245–270–275–275–270–245–230 °C (from the feeding to die zone), a screw speed of 120 rpm and a residence time of about 4 min. The extrudate was then cooled in a water bath, pelletized and vacuum dried for about 10 h at 90 °C. The resulting materials were then compression moulded at 280 °C applying a pressure of 5 bar. The SEM micrographs of the filled and unfilled blends are shown in Fig. 19(a and b). In the unfilled alloy, PET was the minor component and it was present in spherical droplets having mean size of 4.4 μm dispersed in a polyolefin matrix, while HDPE (with a corrugated texture) and PP (with a smoother profile) phases were organized in a co-continuous microstructure. Moreover, PET domains were preferentially localized in the PP component. Nanoclay addition strongly affected the resulting microstructure, leading to an important morphology refinement and to the apparent disappearance of the PET droplets. Moreover, also the characteristic size of the co-continuous domains decreased, rendering thus their identification in the blend more difficult and evidencing a better interpenetration and compatibility between the HDPE and PP phases. The microstructural changes promoted by the nanoclay addition led to a noticeable increase of the softening temperature (>50 °C).

In the paper of Garofalo et al. a recycled material obtained from post-consumer flexible packaging of small size (Fil-s), constituted by PE and smaller concentrations of PP, together with traces of polar contaminants, was nanofilled with small contents (5 wt%) of organoclay [151]. Fil-s and nanoclay were vacuum dried in a oven at 70 °C for 18 h, and then compounded using a twin-screw extruder equipped with co-rotating intermeshing screws. A screw speed of 100 rpm and temperatures of 190 °C, along the barrel, and 160 °C, at the die, were used. Extruded materials were cooled into a water bath and pelletized. The grafting reaction of Fil-s with maleic anhydride was carried out with the same twin-screw extruder. Before the processing, Fil-s granules were mixed with different amounts of maleic anhydride and dicumyl peroxide, previously dissolved in acetone to allow their homogeneous distribution on the granules surfaces. Then, the solvent was let to evaporate under fume-hood for 60 min. The temperature profile of the extruder was set at 190–200–200–190190–165–145–125 °C (from hopper to die) and two different screw speeds (25 and 50 rpm) were considered. Extruded materials were cooled into a water bath and pelletized. Finally, the resulting pellets were processed in the form of ribbons, using a single-screw extruder operating at 40 rpm and at a temperature profile of 220–220–190 °C (from hopper to die). Nanoclay addition led to an interesting stiffness increase, while the reactive functionalization of Fil-s with maleic anhydride led to an improved nanofiller dispersion and compatibility between the polymeric components, with a two-fold increase of the elongation at break. A further increase of the nanoclay content into the maleic anhydride grafted Fil-s allowed to further enhance the elastic modulus of the resulting material.

In a paper of Mistretta et al. PA6/low density polyethylene (LDPE)/organoclay nanocomposites were subjected to multiple reprocessing cycles, with the aim to evaluate the effect of the thermo-mechanical degradation on the rheological and mechanical properties of these blends [157]. The raw materials were premixed in the solid state, keeping a fixed PA6/LDPE ratio of 25/75 wt%, and then processed by using a corotating modular twin screw extruder having multiple input/output along the screw barrel, setting a temperature profile of 180–200–210–220–230–240–240 °C and a screw speed of 220 rpm. The extrudates were then cooled on line in a water bath and pelletized. The reprocessing steps were carried out with a single screw extruder with a thermal profile of 180/200/220/240 °C and at a screw speed of 60 rpm. For comparison, part of the extrudate was processed in a batch mixer for 1 h at 240 °C, setting two different speeds (30 and 60 rpm). All the specimens for the characterization activity were vacuum dried for 3 h at 120 °C and then compression moulded at 240 °C, applying a pressure of 100 bar for 7 min. It was highlighted that the reprocessing behavior was strongly dependent on the processing conditions, on the degradation of each component, and on the specific interactions between the degradation products. These blends were characterized by complex thermo-mechanical mechanisms, such as the degradation of the clay organic modifier (due to Hoffman's elimination reactions) and the degradation of the matrix (characterized by branching and crosslinking reactions). It was demonstrated that under mild reprocessing conditions the blend degradation and the deterioration of the mechanical properties after four extrusion cycles were rather limited, while adopting more severe processing

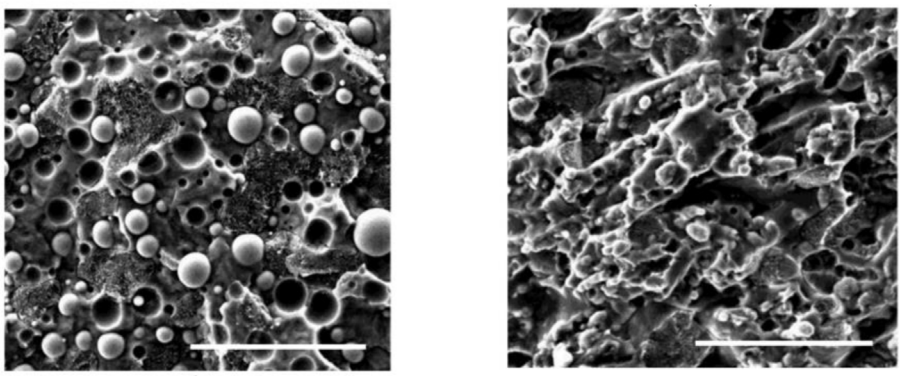

Fig. 19. SEM micrographs of (a) unfilled and (b) organoclay filled (2 phr) HDPE/PP/PET blends. Scale bars represent 50 μm (reprinted with permission from Ref. [156]).

parameters a much more significant deterioration occurred, due to the degradation of the organoclay modifier.

6. Conclusions and future perspectives

This review highlighted the importance of the compatibilization of polymer blends in the modern plastics technology, as it is able to transform a mixture of polymers into an alloy with optimized morphology and suitable, stable, tailorable and reproducible performances. This work briefly presented the most important methods utilized for polymer alloys compatibilization, with particular attention to a recent approach, based on the insertion of nanostructured inorganic materials (mainly nanoclays and carbonaceous nanofillers). It was demonstrated that a proper choice of the nanofillers, also in the presence of a surface modification, can provide an efficient compatibilizing action in incompatible polymer alloys. Several examples of nanocomposite systems based on thermoplastic, thermosetting and elastomeric blends where thus presented, highlighting the strong correlation between the microstructural features and the physical properties of the prepared materials. It was demonstrated that the introduction of these nanofillers can improve the blend interfacial strength, reduce the interfacial tension and refine the morphology by suppressing the coalescence tendency of the dispersed phase, allowing thus the production of high performance and multifunctional nanocomposites that could be applied in a wide range of applications. Moreover, it was shown that the compatibilizing action provided by the nanofillers depends by a complex interplay between thermodynamic and kinetic factors, like the adopted processing conditions, the interaction between fillers and polymer components, the dispersion and localization of these fillers in the blend microstructure. Nanofiller incorporation within polymer blends can also substantially affect their crystallization behavior. Also the intrinsic properties of the nanofillers (i.e., shape, size distribution, aspect ratio, etc.) and the adopted synthesis conditions can strongly influence their compatibilization action in polymer alloys.

Considering the emerging importance of biopolymers and of their relative blends in the modern plastic industry, this review highlighted how nanofiller induced compatibilization approach could be successfully extended also to bioplastics-based alloys. However, if biodegradable materials are utilized, the biodegradability of resulting blends should be carefully assessed. Moreover, considering also the environmental concerns on the management of plastic waste an on the recycling of traditional plastics, this review showed that nanomodification of recycled polymers could lead to the development of recyclates with better compatibility and higher physical properties, even in the presence of multiple polymeric phases.

However, nanofiller induced compatibilization in polymer blends is still a novel technology, and many efforts should be made in the future to have a detailed comprehension of the physical and chemical aspects involved in this technique. For instance, it will be important to apply novel experimental approaches to investigate the orientation of the nanofiller in the interfacial region, and how the macromolecular dynamics and the interfacial thickness are influenced by the presence of the nanoparticles. Also the role played by the melt rheology of the polymer components on the preferential localization of the nanoparticles should be better analyzed. Moreover, the possibility of in-situ detecting the localization and the dispersion of the nanoparticles during the processing could be important in the future to tailor and further increase the performances of nanocomposite polymer alloys, also by limiting as much as possible the nanofiller content.

Declaration of competing interest

The authors declare that they have no known competing financial interests or personal relationships that could have appeared to influence the work reported in this paper.

References

[1] G. Fredi, A. Dorigato, Recycling of bioplastic waste: a review, Adv. Ind. Eng. Polym. Res. 4 (2021) 159–177.
[2] L.A. Utracki, Polymer Blends Handbook, Kluwer academic publishers, 2002.
[3] L.A. Utracki, Commercial Polymer Blends, Springer US, 1998.
[4] A. Dorigato, A. Pegoretti, L. Fambri, C. Lonardi, M. Slouf, J. Kolarik, Linear low density polyethylene - cycloolefin copolymer blends, Express Polym. Lett. 5 (1) (2011) 23–37.
[5] Z. Horak, I. Fortelny, J. Kolarik, D. Hlavata, A. Sikora, Polymer blends, in: Encyclopedia of Polymer Science and Technology, John Wiley & Sons Inc., 2005.
[6] F.P. La Mantia, M. Morreale, L. Botta, M.C. Mistretta, M. Ceraulo, R. Scaffaro, Degradation of polymer blends: a brief review, Polym. Degrad. Stabil. 145 (2017) 79–92.
[7] B.D. Gesner, Encyclopedia of Polymer Science and Technology, vol. 10, Interscience, New York, 1969.
[8] A.R. Ajitha, L.P. Mathew, S. Thomas, Compatibilization of polymer blends by micro and nanofillers, in: Compatibilization of Polymer Blends: Micro and Nano Scale Phase Morphologies, Interphase Characterization, and Properties, 2019, pp. 179–203.
[9] L.A. Utracki, Polymer Alloys and Blends, Thermodynamic and Rheology, Hanser Publishers, Munich (Germany), 1989.
[10] P.J. Flory, Principles of Polymer Chemistry, Cornell University Press, Ithaca (New York), 1953.
[11] G.L. Lewis, M. Randall, Thermodynamics, McGraw-Hill, New York, 1961.
[12] I.M. Kalogeras, Glass-transition phenomena in polymer blends, in: A.I. Isayev (Ed.), Encyclopedia of Polymer Blends, vol. 3, Structure, Wiley-VCH Verlag GmbH & Co. KGaA, Weinheim (Germany), 2016, pp. 1–134.
[13] Y. Deng, C. Yu, P. Wongwiwattana, N.L. Thomas, Optimising ductility of poly(lactic acid)/poly(butylene adipate-co-terephthalate) blends through Co-continuous phase morphology, J. Polym. Environ. 26 (9) (2018) 3802–3816.
[14] B.D. Favis, in: D.R. Paul, C.B. Bucknall (Eds.), Polymer Blends, vol. 1, Formulations, John Wiley & Sons Inc., New York, 2000.
[15] H. Van Oene, in: D.R. Paul, S. Newman (Eds.), Polymer Blends, vol. 2, Academic Press Inc., New York, 1978.
[16] R. Scaffaro, L. Botta, M.C. Mistretta, F.P. La Mantia, Processing – morphology – property relationships of polyamide 6/polyethylene blend–clay nanocomposites, Express Polym. Lett. 7 (10) (2013) 873–884.
[17] L.A. Utracki, Compatibilization of polymer blends, Can. J. Chem. Eng. 80 (6) (2002) 1008–1016.
[18] D.R. Paul, S. Newman, Polymer Blends, vols. 1–2, Academic Press Inc., New York, 1978.
[19] A. Ryan, Designer polymer blends, Nat. Mater. 1 (2002) 8–10.
[20] D. Rajasekaran, P.K. Maji, Recycling of plastic wastes with poly (ethylene-co-methacrylic acid) copolymer as compatibilizer and their conversion into high-end product, Waste Manage. 74 (2018) 135–143.
[21] B. Imre, L. Garcia, D. Puglia, F. Vilaplana, Reactive compatibilization of plant polysaccharides and biobased polymers: review on current strategies, expectations and reality, Carbohydr. Polym. 209 (2019) 20–37.
[22] R. Fayt, R. Jerome, P. Teyssie, Characterization and control of interfaces in emulsified incompatible polymer blends, Polym. Eng. Sci. 27 (1987) 328–334.
[23] K.R. Srinivasan, A.K. Gupta, Mechanical properties and morphology of PP/SEBS/PC blends, J. Appl. Polym. Sci. 53 (1994) 1.
[24] R. Fayt, R. Jerome, P. Teyssie, Molecular design of multicomponent polymer systems. XII. Direct observation of the location of a block compolymer in low-density polyethylene-polystyrene blends, J. Polym. Sci. Polym. Lett. Ed. 24 (1986) 25–28.
[25] R. Fayt, R. Jerome, P. Teyssie, Molecular design of multicomponent polymer systems, XIII. Control of the morphology of polyethylene/polystyrene blends by block copolymers, Makromol. Chem. 187 (1986) 837–852.
[26] R. Fayt, R. Jerome, P. Teyssie, Molecular design of multicomponent polymer systems. XIV. Control of the mechanical properties of polyethylene–polystyrene blends by block copolymers, J. Polym. Sci., Part B: Polym. Phys. 27 (1989) 775–793.
[27] H.G. Lee, Y.T. Sung, Y.K. Lee, W.N. Kim, H.G. Yoon, H.S. Lee, Effects of PP-g-MAH on the mechanical, morphological and rheological properties of polypropylene and poly(acrylonitrile-butadiene-styrene) blends, Macromol. Res. 17 (6) (2009) 417–423.
[28] P. Singh, P. Katiyar, H. Singh, Impact of compatibilization on polypropylene (PP) and acrylonitrile butadiene styrene (ABS) blend: a review, Mater. Today: Proc. 78 (1) (2023) 189–197.

[29] C.L. Zhang, L.F. Feng, X.P. Gu, S. Hoppe, G.H. Hu, Efficiency of graft copolymers as compatibilizers for immiscible polymer blends, Polymer 48 (20) (2007) 5940–5949.
[30] C.L. Zhang, L.F. Feng, X.P. Gu, S. Hoppe, G.H. Hu, Blend composition dependence of the compatibilizing efficiency of graft copolymers for immiscible polymer blends, Polym. Eng. Sci. 50 (11) (2010) 2243–2251.
[31] S. Yukioka, T. Inoue, Ellipsometric studies on immiscible polymer-polymer interfaces, Polymer 34 (1993) 1256–1259.
[32] S. Yukioka, T. Inoue, Ellipsometric analysis on the in situ reactive compatibilization of immiscible polymer blends, Polymer 35 (1994) 1182–1186.
[33] J. Kressler, N. Higashida, T. Inoue, W. Heckmann, F. Seitz, Study of polymer-polymer interfaces: a comparison of ellipsometric and TEM data of PMMA/polystyrene and PMMA/SAN systems, Macromolecules 26 (1993) 2090–2094.
[34] S. Al Malaika, Reactive Modifiers for Polymers, Chapman & Hall, London, 1997.
[35] W.E. Baker, C. Scott, G.H. Hu, Reactive Polymer Blending, Carl Hanser Verlag, Munich, 2001.
[36] Z. Krulis, Z. Horak, F. Lednicky, J. Pospisil, M. Sufcak, Reactive compatibilization of polyolefins using low molecular weight polybutadiene, Angew. Makromol. Chem. 258 (1998) 63.
[37] H.X. Zhang, D.J. Hourston, Reactive compatibilization of poly(butylene terephthalate)/low-density polyethylene and poly(butylene terephthalate)/ethylene propylene diene rubber blends with a bismaleimide, J. Appl. Polym. Sci. 71 (1999) 2049–2057.
[38] J. Schies, D.B. Priddy, Modern Styrenic Polymers: Polystyrene and Styrenic Copolymers, John Wiley & Sons, Chichester (UK), 2003.
[39] Y.J. Sun, G.H. Hu, M. Lambla, Melt free-radical grafting of glycidyl methacrylate onto polypropylene, Angew. Makromol. Chem. 229 (1) (1995) 1–13.
[40] H.Z. He, S.M. Liu, Y.P. Ni, F. Xue, B. Xue, Z.W. Zhu, Z.X. Huang, Fabrication of poly(ethylene terephthalate)/polypropylene-based elastomer blends with balanced stiffness-toughness: the effect of reactive compatibilization, J. Thermoplast. Compos. Mater. 35 (12) (2020) 2465–2480.
[41] G.H. Hu, H. Cartier, C. Plummer, Reactive extrusion: toward nanoblends, Macromolecules 32 (1999) 4713–4718.
[42] G.H. Hu, H. Cartier, L.F. Feng, B.G. Li, Kinetics of the in situ polymerization and in situ compatibilization of poly(propylene) and polyamide 6 blends, J. Appl. Polym. Sci. 91 (2004) 1498–1504.
[43] G.H. Hu, H. Li, L.F. Feng, Follow-up of the course of the anionic ring-opening polymerization of lactams onto an isocyanate-bearing polymer backbone in the melt, J. Appl. Polym. Sci. 102 (5) (2006) 4394–4403.
[44] A. Carbonell-Verdu, J.M. Ferri, F. Dominici, T. Boronat, L. Sanchez-Nacher, R. Balart, L. Torre, Manufacturing and compatibilization of PLA/PBAT binary blends by cottonseed oil-based derivatives, Express Polym. Lett. 12 (9) (2018) 808–823.
[45] M.J. Garcia-Campo, L. Quiles-Carrillo, J. Masia, M.J. Reig-Perez, N. Montanes, R. Balart, Environmentally friendly compatibilizers from soybean oil for ternary blends of poly(lactic acid)-PLA, poly(epsilon-caprolactone)-PCL and poly(3-hydroxybutyrate)-PHB, Materials 10 (11) (2017) 1339.
[46] H. Hu, A. Xu, D. Zhang, W. Zhou, S. Peng, X. Zhao, High-toughness poly(lactic acid)/starch blends prepared through reactive blending plasticization and compatibilization, Molecules 25 (24) (2020) 5951.
[47] L. Quiles-Carrillo, O. Fenollar, R. Balart, S. Torres-Giner, M. Rallini, F. Dominici, L. Torre, A comparative study on the reactive compatibilization of melt-processed polyamide 1010/polylactide blends by multi-functionalized additives derived from linseed oil and petroleum, Express Polym. Lett. 14 (6) (2020) 583–604.
[48] I. Dominguez-Candela, J. Gomez-Caturla, S.C. Cardona, J. Lora-García, V. Fombuena, Novel compatibilizers and plasticizers developed from epoxidized and maleinized chia oil in composites based on PLA and chia seed flour, Eur. Polym. J. 173 (2022) 111289.
[49] J. Gomez-Caturla, I. Dominguez-Candela, M.P. Medina-Casas, J. Ivorra-Martinez, V. Moreno, R. Balart, D. Garcia-Garcia, Improvement of poly(lactide) ductile properties by plasticization with biobased tartaric acid ester, Macromol. Mater. Eng. 308 (7) (2023) 2200694.
[50] P. Liminana, L. Quiles-Carrillo, T. Boronat, R. Balart, N. Montanes, The effect of varying almond shell flour (ASF) loading in composites with poly(butylene succinate (PBS) matrix compatibilized with maleinized linseed oil (MLO), Materials 11 (11) (2018) 2179.
[51] X. Ren, K. Li, Investigation of vegetable-oil-based coupling agents for kenaf-fiber-reinforced unsaturated polyester composites, J. Appl. Polym. Sci. 128 (2) (2013) 1101–1109.
[52] V. Shifrin, Y.S. Lipatov, A.Y. Nesterov, The introduction of a filler and consequent increase in the thermodynamic compatibility of binary polyblends, Polym. Sci. 27 (2) (1985) 412–417.
[53] A. Karim, D.W. Liu, J.F. Douglas, A. Nakatani, E.J. Amis, Modification of the phase stability of polymer blends by fillers, Polymer 41 (23) (2004) 8455–8458.
[54] Y. Huang, S. Jiang, G. Li, D. Chen, Effect of fillers on the phase stability of binary polymer blends: a dynamic shear rheology study, Acta Mater. 53 (19) (2005) 5117–5124.
[55] H. Ishida, N. Scherbakoff, Interphase compatibilization of composites with immiscible blends as matrix: glass beads filled nylon 6/polypropylene blend-composite, Makromol. Chem. Macromol. Symp. 50 (1) (1991) 157–170.
[56] A. Pegoretti, A. Dorigato, Polymer composites: reinforcing fillers, in: Encyclopedia of Polymer Science and Technology, 2019, pp. 1–72.
[57] P.M. Ajayan, L.S. Schadler, P.V. Braun, Nanocomposite Science and Technology, Wiley-VCH Verlag GmbH & Co. KGaA, Weinheim (Germany), 2003.
[58] S. Das, S.K. Samal, S. Mohanty, S.K. Nayak, Crystallization of polymer blend nanocomposites, in: Crystallization in Multiphase Polymer Systems, 2018, pp. 313–339.
[59] M. Yousfi, S. Livi, A. Dumas, J. Crépin-Leblond, M. Greenhill-Hooper, J. Duchet-Rumeau, Compatibilization of polypropylene/polyamide 6 blends using new synthetic nanosized talc fillers: morphology, thermal, and mechanical properties, J. Appl. Polym. Sci. 131 (13) (2014) 40453.
[60] A. Nesterov, Y. Lipatov, Compatibilizing effect of a filler in binary polymer mixtures, Polymer 40 (5) (1999) 1347–1349.
[61] V.V. Ginzburg, Influence of nanoparticles on miscibility of polymer blends. A simple theory, Macromolecules 38 (6) (2005) 2362–2367.
[62] J. Vermant, G. Cioccolo, K.G. Nair, P. Moldenaers, Coalescence suppression in model immiscible polymer blends by nano-sized colloidal particles, Rheol. Acta 43 (5) (2004) 529–538.
[63] S. George, K. Ramamurthy, J. Anand, G. Groeninckx, K. Varughese, S. Thomas, Rheological behaviour of thermoplastic elastomers from polypropylene/acrylonitrileebutadiene rubber blends: effect of blend ratio, reactive compatibilization and dynamic vulcanization, Polymer 40 (15) (1999) 4325–4344.
[64] R. Salehiyan, H.Y. Song, M. Kim, W.J. Choi, K. Hyun, Morphological evaluation of PP/PS blends filled with different types of clays by nonlinear rheological analysis, Macromolecules 49 (8) (2016) 3148–3160.
[65] J. Chen, X.C. Du, W.B. Zhang, J.H. Yang, N. Zhang, T. Huang, Y. Wang, Synergistic effect of carbon nanotubes and carbon black on electrical conductivity of PA6/ABS blend, Compos. Sci. Technol. 81 (2013) 1–8.
[66] J. Chen, Y.Y. Shi, J.H. Yang, N. Zhang, T. Huang, C. Chen, Y. Wang, Z.W. Zhou, A simple strategy to achieve very low percolation threshold via the selective distribution of carbon nanotubes at the interface of polymer blends, J. Mater. Chem. 22 (42) (2012) 22398–22404.
[67] D. Wu, Y. Sun, D. Lin, W. Zhou, M. Zhang, L. Yuan, Selective localization behavior of carbon nanotubes: effect on transesterification of immiscible polyester blends, Macromol. Chem. Phys. 212 (15) (2011) 1700–1709.
[68] Y. Son, Measurement of interface free energy in polypropylene/ethylene-propylene rubber blends, J. Adhes. 9 (12) (2015) 909–919.
[69] S. Nuriel, L. Liu, A. Barber, H. Wagner, Direct measurement of multiwall nanotube surface tension, Chem. Phys. Lett. 404 (4) (2005) 263–266.
[70] S.T. Nair, P.P. Vijayan, P. Xavier, S. Bose, S.C. George, S. Thomas, Selective localisation of multi walled carbon nanotubes in polypropylene/natural rubber blends to reduce the percolation threshold, Compos. Sci. Technol. 116 (2015) 9–17.
[71] M.H. Al-Saleh, Carbon nanotube-filled polypropylene/polyethylene blends: compatibilization and electrical properties, Polym. Bull. 73 (4) (2016) 975–987.
[72] H.J. Chung, J. Kim, K. Ohno, R.J. Composto, Controlling the location of nanoparticles in polymer blends by tuning the length and end group of polymer brushes, ACS Macro Lett. 1 (1) (2011) 252–256.
[73] A. Göldel, A. Marmur, G.R. Kasaliwal, P. Pötschke, G. Heinrich, Shape-dependent localization of carbon nanotubes and carbon black in an immiscible polymer blend during melt mixing, Macromolecules 44 (15) (2011) 6094–6102.
[74] I. Otero-Navas, M. Arjmand, U. Sundararaj, Carbon nanotube induced double percolation in polymer blends: morphology, rheology and broadband dielectric properties, Polymer 114 (2017) 122–134.
[75] Y. Shen, T.T. Zhang, J.H. Yang, N. Zhang, T. Huang, Y. Wang, Selective localization of reduced graphene oxides at the interface of PLA/EVA blend and its resultant electrical resistivity, Polym. Compos. 38 (9) (2017) 1982–1991.
[76] X. Zhao, J. Zhao, J.P. Cao, D. Wang, G.H. Hu, F. Chen, Z.M. Dang, Effect of the selective localization of carbon nanotubes in polystyrene/poly (vinylidene fluoride) blends on their dielectric, thermal, and mechanical properties, Mater. Des. 56 (2014) 807–815.
[77] T. Zhang, J. Yang, N. Zhang, T. Huang, Y. Wang, Achieving large dielectric property improvement in poly (ethylene vinyl acetate)/thermoplastic polyurethane/multiwall carbon nanotube nanocomposites by tailoring phase morphology, Ind. Eng. Chem. Res. 56 (13) (2017) 3607–3617.
[78] F.X. Liang, C.L. Zhang, Z.Z. Yang, Rational design and synthesis of Janus composites, Adv. Mater. 26 (2014) 6944–6949.
[79] Y. Hou, G.L. Zhang, X.P. Tang, Y. Si, X.M. Song, F.X. Liang, Z.Z. Yang, Janus nanosheets synchronously strengthen and toughen polymer blends, Macromolecules 52 (2019) 3863–3868.
[80] H.L. He, F.X. Liang, Interfacial engineering of polymer blend with Janus particle as compatibilizer, Chin. J. Polym. Sci. 41 (2023) 500–515.
[81] M. Salzano de Luna, G. Filippone, Effects of nanoparticles on the morphology of immiscible polymer blends – challenges and opportunities, Eur. Polym. J. 79 (2016) 198–218.
[82] A. Taguet, P. Cassagnau, J.M. Lopez-Cuesta, Structuration, selective dispersion and compatibilizing effect of (nano)fillers in polymer blends, Prog. Polym. Sci. 39 (8) (2014) 1526–1563.
[83] M. Liebscher, M.O. Blais, P. Pötschke, G. Heinrich, A morphological study on the dispersion and selective localization behavior of graphene nanoplatelets in immiscible polymer blends of PC and SAN, Polymer 54 (2013) 5875–5882.

[84] P. Mederic, J. Ville, J. Huitric, M. Moan, T. Aubry, Effect of processing procedures and conditions on structural, morphological, and rheological properties of polyethylene/polyamide/nanoclay blends, Polym. Eng. Sci. 51 (2011) 969–978.
[85] F. Gubbels, R. Jerome, E. Vanlathem, R. Deltour, S. Blacher, F. Brouers, Kinetic and thermodynamic control of the selective localization of carbon black at the interface of immiscible polymer blends, Chem. Mater. 10 (1998) 1227–1235.
[86] S.T. Knauert, J.F. Douglas, F.W. Starr, The effect of nanoparticle shape on polymer-nanocomposite rheology and tensile strength, J. Polym. Sci., Part B: Polym. Phys. 45 (2007) 1882–1897.
[87] M.J.A. Hore, M. Laradji, Prospects of nanorods as an emulsifying agent of immiscible blends, J. Chem. Phys. 128 (2008) 54901–54908.
[88] S. Sinha Ray, S. Pouliot, M. Bousmina, L.A. Utracki, Role of organically modified layered silicate as an active interfacial modifier in immiscible polystyrene/polypropylene blends, Polymer 45 (2004) 8403–8413.
[89] W. Zhang, M. Lin, A. Winesett, O. Dhez, A.L. Kilcoyne, H. Ade, M. Rubinstein, K.V.P.M. Shafi, A. Ulman, D. Gersappe, R. Tenne, M. Rafailovich, J. Sokolov, H.L. Frisch, The use of functionalized nanoparticles as non-specific compatibilizers for polymer blends, Polym. Adv. Technol. 22 (1) (2011) 65–71.
[90] M.E. Mackay, A. Tuteja, P.M. Duxbury, C.J. Hawker, B. Van Horn, Z. Guan, G. Chen, R.S. Krishnan, General strategies for nanoparticle dispersion, Science 311 (2006) 1740–1743.
[91] A. Kelarakis, E.P. Giannelis, K. Yoon, Structure–properties relationships in clay nanocomposites based on PVDF/(ethylene–vinylacetate) copolymer blends, Polymer 48 (2007) 7567–7572.
[92] Z. Hrnjak-Murgic, Z. Jelcic, V. Kovacevic, M. Mlinac-Misak, J. Jelencic, Molecular and morphological characterization of immiscible SAN/EPDM blends filled by nanofiller, Macromol. Mater. Eng. 287 (2002) 684–692.
[93] A. Walther, K. Matussek, A.H.E. Müller, Engineering nanostructured polymer blends with controlled nanoparticle location using Janus particles, ACS Nano 2 (2008) 1167–1178.
[94] F. Hemmati, H. Garmabi, H. Modarress, Compatibilization mechanisms of nanoclays with different surface modifiers in UCST blends: opposing effects on phase miscibility, Polymer 55 (25) (2014) 6623–6633.
[95] F. Hemmati, H. Garmabi, H. Modarress, Effects of organoclay on the compatibility and interfacial phenomena of PE/EVA blends with UCST phase behavior, Polym. Compos. 35 (12) (2014) 2329–2342.
[96] M. Jorda-Reolid, V. Moreno, A. Martinez-Garcia, J.A. Covas, J. Gomez-Caturla, J. Ivorra-Martinez, L. Quiles-Carrillo, Incorporation of argan shell flour in a biobased polypropylene matrix for the development of high environmentally friendly composites by injection molding, Polymers 15 (12) (2023) 2743.
[97] P.A. da Silva, M.M. Jacobi, L.K. Schneider, R.V. Barbosa, P.A. Coutinho, R.V.B. Oliveira, R.S. Mauler, SBS nanocomposites as toughening agent for polypropylene, Polym. Bull. 64 (3) (2009) 245–257.
[98] N. Chandran, S. Chandran, H.J. Maria, S. Thomas, Compatibilizing action and localization of clay in a polypropylene/natural rubber (PP/NR) blend, RSC Adv. 5 (105) (2015) 86265–86273.
[99] M.J. Azizl, M. Barghamadi, K. Rezaeeparto, M. Mokhtary, S. Parham, Graphene oxide and graphene hybrid nanocomposites based on compatibilized PP/PTW/EVA: effect of nanofiller and compatibilizer on the modeling of viscoplastic behavior, J. Polym. Res. 28 (8) (2021) 293.
[100] H. Panigrahi, D.K. K, Jamming carbonaceous nanofiller in the continuous phase and at the blend interface for phenomenal improvement in the overall physico-mechanical properties of compatibilized thermoplastic elastomer, Polymer 257 (2022) 125261.
[101] D. Pedrazzoli, A. Dorigato, T. Conti, L. Vanzetti, M. Bersani, A. Pegoretti, Liquid crystalline polymer nanocomposites reinforced with in-situ reduced graphene oxide, Express Polym. Lett. 9 (8) (2015) 709–720.
[102] V. Moreno, K. Murtada, M. Zougagh, Á. Ríos, Analytical control of Rhodamine B by SERS using reduced graphene decorated with copper selenide, Spectrochim. Acta, Part A 223 (2019) 117302.
[103] Z. Evgeni, T. Roza, M. Narkis, S. Arnon, Particulate multi-phase polymeric nanocomposites, Polym. Compos. 27 (4) (2006) 425–430.
[104] S.M.R. Paran, M. Abdorahimi, A. Shekarabi, H.A. Khonakdar, S.H. Jafari, M.R. Saeb, Modeling and analysis of nonlinear elastoplastic behavior of compatibilized polyolefin/polyester/clay nanocomposites with emphasis on interfacial interaction exploration, Compos. Sci. Technol. 154 (2018) 92–103.
[105] J.M. Feng, X.Q. Liu, R.Y. Bao, W. Yang, B.H. Xie, M.B. Yang, Suppressing phase coarsening in immiscible polymer blends using nano-silica particles located at the interface, RSC Adv. 5 (91) (2015) 74295–74303.
[106] Y. Wang, Q. Zhang, Q. Fu, Compatibilization of immiscible poly (propylene)/polystyrene blends using clay, Macromol. Rapid Commun. 24 (3) (2003) 231–235.
[107] M.S. Thompson, S. Agarwal, R.K. Gupta, Effects of extensional flow and nanofiller incorporation on dispersed phase size in the blending of high-viscosity-ratio immiscible vinyl polymers, J. Vinyl Addit. Technol. 28 (1) (2021) 104–114.
[108] O.M. Istrate, M.A. Gunning, C.L. Higginbotham, B. Chen, Structure-property relationships of polymer blend/clay nanocomposites: compatibilized and noncompatibilized polystyrene/propylene/clay, J. Polym. Sci., Part B: Polym. Phys. 50 (6) (2012) 431–441.
[109] C.B.B. Luna, E. da Silva Barbosa Ferreira, D.D. Siqueira, E.M. Araújo, E.P. do Nascimento, E.S. Medeiros, T.J.A. de Mélo, Electrical nanocomposites of PA6/ABS/ABS-MA reinforced with carbon nanotubes (MWCNTf) for antistatic packaging, Polym. Compos. 43 (6) (2022) 3639–3658.
[110] Y. Cao, J. Zhang, J. Feng, P. Wu, Compatibilization of immiscible polymer blends using graphene oxide sheets, ACS Nano 5 (7) (2011) 5920–5927.
[111] L. Guo, Y. Xu, X. Zhang, G.H. Hu, In-situ compatibilization of polyamide 6/polycarbonate blends through interfacial localization of silica nanoparticles, Polymer 274 (2023) 125898.
[112] M. Yousfi, J. Soulestin, B. Vergnes, M.F. Lacrampe, P. Krawczak, Morphology and mechanical properties of PET/PE blends compatibilized by nanoclays: effect of thermal stability of nanofiller organic modifier, J. Appl. Polym. Sci. 128 (5) (2013) 2766–2778.
[113] M. Yousfi, J. Soulestin, B. Vergnes, M.F. Lacrampe, P. Krawczak, Compatibilization of immiscible polymer blends by organoclay: effect of nanofiller or organo-modifier? Macromol. Mater. Eng. 298 (7) (2013) 757–770.
[114] R.H. Pour, A. Hassan, M. Soheilmoghaddam, H.C. Bidsorkhi, Mechanical, thermal, and morphological properties of graphene reinforced polycarbonate/acrylonitrile butadiene styrene nanocomposites, Polym. Compos. 37 (2016) 1633.
[115] R.H. Pour, M. Soheilmoghaddam, A. Hassan, S. Bourbigot, Flammability and thermal properties of polycarbonate/acrylonitrile-butadiene-styrene nanocomposites reinforced with multilayer graphene, Polym. Degrad. Stabil. 120 (2015) 88–97.
[116] W. Yu, H. Xie, L. Chen, M. Wang, W. Wang, Synergistic thermal conductivity enhancement of PC/ABS composites containing alumina/magnesia/graphene nanoplatelets, Polym. Compos. 38 (2017) 2221–2227.
[117] J.Y. Park, B.Y. Lee, H.J. Cha, Y.C. Kim, Effects of compatibilizer and graphene oxide on the impact strength of PC/ABS blend, Appl. Chem. Eng. 26 (2015) 173–177.
[118] E.G.R. Anjos, L. Souza Vieira, J. Marini, T.R. Brazil, N.A.S. Gomes, M.C. Rezende, F.R. Passador, Influence of graphene nanoplates and ABS-g-MAH on the thermal, mechanical, and electromagnetic properties of PC/ABS blend, J. Appl. Polym. Sci. 139 (3) (2021) 51500.
[119] S. Sinha Ray, M. Bousmina, Compatibilization efficiency of organoclay in an immiscible polycarbonate/poly (methyl methacrylate) blend, Macromol. Rapid Commun. 26 (6) (2005) 450–455.
[120] I. Taraghi, A. Fereidoon, S. Paszkiewicz, Z. Roslaniec, Nanocomposites based on polymer blends: enhanced interfacial interactions in polycarbonate/ethylene-propylene copolymer blends with multi-walled carbon nanotubes, Compos. Interfac. 25 (3) (2018) 275–286.
[121] D. Vrsaljko, X. Bao, Compatibilization of PUR/PVAC polymer blend by addition of calcium carbonate filler, Polym. Compos. 37 (4) (2016) 1274–1281.
[122] M. Mohamadi, M. Papila, H. Garmabi, Z. Gohari Bajestani, Morphological evaluation and phase behavior of PVDF/PEO blends in the presence of graphene nanoplatelets through rheological measurements, J. Appl. Polym. Sci. 136 (40) (2019) 48017.
[123] A. Torabi, S.H. Jafari, H.A. Khonakdar, V. Goodarzi, L. Yu, A.L. Skov, Electroactive phase enhancement in poly(vinylidene fluoride-hexafluoropropylene)/polycarbonate blends by hybrid nanofillers, J. Appl. Polym. Sci. 139 (12) (2021) 51825.
[124] N. Lopattananon, J. Julyanon, A. Masa, A. Kaesaman, C. Thongpin, T. Sakai, The role of nanofillers on (natural rubber)/(ethylene vinyl acetate)/clay nanocomposite in blending and foaming, J. Vinyl Addit. Technol. 21 (2) (2015) 134–146.
[125] N. Ashok, D. Webert, P.V. Suneesh, M. Balachandran, Mechanical and sorption behaviour of organo-modified montmorillonite nanocomposites based on EPDM – NBR Blends, Mater. Today: Proc. 5 (8) (2018) 16132–16140.
[126] Z. Eslami, M. Mirzapour, Compatibilizing effect and reinforcing efficiency of nanosilica on ethylene-propylene diene monomer/chloroprene rubber blends, Polym. Compos. 42 (4) (2021) 1809–1817.
[127] Y. Li, S. Wang, Y. Zhang, Y. Zhang, Crystallization behavior of carbon black-filled polypropylene and polypropylene/epoxy composites, J. Appl. Polym. Sci. 102 (2006) 104–118.
[128] A.M. Díez-Pascual, P.S. Shuttleworth, E.I. Gónzalez-Castillo, C. Marco, M.A. Gómez-Fatou, G. Ellis, Polymer blend nanocomposites: effect of selective nanotube location on the properties of a semicrystalline thermoplastic-toughened epoxy thermoset, Macromol. Mater. Eng. 299 (12) (2014) 1430–1444.
[129] M.M. Salehi, H. Nazockdast, G.R. Pircheraghi, The role of organoclay on microstructure development and rheological properties of poly(butylene terephtalate)/epoxy/organoclay hybrid systems, J. Macromol. Sci. B 51 (2012) 906–925.
[130] A. Vyas, J.O. Iroh, Clay induced thermoplastic crystals in thermoset matrix: thermal, dynamic mechanical, and morphological analysis of clay/nylon-6-epoxy nanocomposites, Polym. Compos. 37 (2016) 2206–2217.
[131] D. Garlotta, A literature review of poly(lactic acid), J. Polym. Environ. 9 (2) (2001) 63–84.
[132] A. Dorigato, G. Fredi, M. Negri, A. Pegoretti, Thermo-mechanical behaviour of novel wood laminae-thermoplastic starch biodegradable composites with thermal energy storage/release capability, Front. Mater. 6 (2019) 1–12.
[133] S.S. Ray, K. Okamoto, M. Okamoto, Structure-property relationship in biodegradable poly(butylene succinate)/layered silicate nanocomposites, Macromolecules 36 (2003) 2355–2367.
[134] F. Valentini, A. Dorigato, D. Rigotti, A. Pegoretti, Polyhydroxyalkanoates/fibrillated nanocellulose composites for additive manufacturing, J. Polym. Environ. 27 (2019) 1333–1341.

[135] V. Siracusa, I. Blanco, Bio-polyethylene (Bio-PE), bio-polypropylene (Bio-PP) and bio-poly(ethylene terephthalate) (Bio-PET): recent developments in biobased polymers analogous to petroleum-derived ones for packaging and engineering applications, Polymers 12 (8) (2020) 1641.
[136] A.G. de Oliveira, J.F. Moreno, A.M.F. de Sousa, V.A. Escócio, M.J. de Oliveira Cavalcanti Guimarães, A.L.N. da Silva, Composites based on high-density polyethylene, polylactide and calcium carbonate: effect of calcium carbonate nanoparticles as co-compatibilizers, Polym. Bull. 77 (6) (2019) 2889–2904.
[137] G. Fredi, M. Karimi Jafari, A. Dorigato, D.N. Bikiaris, A. Pegoretti, Improving the thermomechanical properties of poly(lactic acid) via reduced graphene oxide and bioderived poly(decamethylene 2,5-furandicarboxylate), Materials 15 (4) (2022) 1316.
[138] A. Barandiaran, J. Gomez-Caturla, J. Ivorra-Martinez, D. Lascano, M.A. Selles, V. Moreno, O. Fenollar, Esters of cinnamic acid as green plasticizers for polylactide formulations with improved ductility, Macromol. Mater. Eng. (2023) 2300022.
[139] A. Bher, I. Uysal Unalan, R. Auras, M. Rubino, C.E. Schvezov, Toughening of poly(lactic acid) and thermoplastic cassava starch reactive blends using graphene nanoplatelets, Polymers 10 (1) (2018) 95.
[140] X. Li, Z. Fu, X. Gu, H. Liu, H. Wang, Y. Li, Interfacially located nanoparticles: barren nanorods versus polymer grafted nanorods, Compos. B Eng. 198 (2020) 108153.
[141] T.T. Thiyagu, G. Gokilakrishnan, V.C. Uvaraja, T. Maridurai, V.R.A. Prakash, Effect of SiO2/TiO2 and ZnO nanoparticle on cardanol oil compatibilized PLA/PBAT biocomposite packaging film, Silicon 14 (7) (2022) 3795–3808.
[142] N. Bitinis, R. Verdejo, E. Maya, E. Espuche, P. Cassagnau, M. Lopez-Manchado, Physicochemical properties of organoclay filled polylactic acid/natural rubber blend bionanocomposites, Compos. Sci. Technol. 72 (2) (2012) 305–313.
[143] H. Wu, A. Hou, J.P. Qu, Phase morphology and performance of supertough PLA/EMA-GMA/ZrP nanocomposites prepared through reactive melt-blending, ACS Omega 4 (21) (2019) 19046–19053.
[144] T.G. Darshan, S. Veluri, B. Kartik, C. Yen-Hsiang, C. Fang-Chyou, Poly(butylene succinate)/high density polyethylene blend-based nanocomposites with enhanced physical properties – selectively localized carbon nanotube in pseudo-double percolated structure, Polym. Degrad. Stabil. 163 (2019) 185–194.
[145] R.J. Ehrig, Plastic Recycling, Carl Hanser Verlag, Munich, 1989.
[146] J. Scheirs, Polymer Recycling, John Wiley & Sons Inc., New York, 1998.
[147] M.N. Subramanian, Polymer Blends and Composites - Chemistry and Technology, John Wiley & Sons, Inc., Hoboken (USA), 2017.
[148] P.M. Visakh, O.B. Nazarenko, Thermal degradation of polymer blends, composites and nanocomposites, in: P. Visakh, Y. Arao (Eds.), Thermal Degradation of Polymer Blends, Composites and Nanocomposites, Springer Cham, 2015.
[149] R. Muthuraj, M. Misra, A.K. Amar Kumar Mohanty, Biodegradable compatibilized polymer blends for packaging applications: a literature review, J. Appl. Polym. Sci. 135 (2018) 45726.
[150] A. Soroudi, I. Jakubowicz, Recycling of bioplastics, their blends and biocomposites: a review, Eur. Polym. J. 49 (10) (2013) 2839–2858.
[151] E. Garofalo, L. Di Maio, P. Scarfato, F. Di Gregorio, L. Incarnato, Reactive compatibilization and melt compounding with nanosilicates of post-consumer flexible plastic packagings, Polym. Degrad. Stabil. 152 (2018) 52–63.
[152] N.S. Nor Arman, R.S. Chen, S. Ahmad, D. Shahdan, Mechanical and physical characterizations of compatibilizer-free recycled plastics blend composites modified with carbon nanotube and clay nanofiller, J. Appl. Polym. Sci. 139 (32) (2022) e52768.
[153] R.S. Chen, S. Ahmad, S. Gan, M.H. Ab Ghani, M.N. Salleh, Effects of compatibilizer, compounding method, extrusion parameters, and nanofiller loading in clay-reinforced recycled HDPE/PET nanocomposites, J. Appl. Polym. Sci. 132 (29) (2015) 42287.
[154] R.S. Chen, M.H. Ab Ghani, M.N. Salleh, S. Ahmad, M.A. Tarawneh, Mechanical, water absorption, and morphology of recycled polymer blend rice husk flour biocomposites, J. Appl. Polym. Sci. 132 (8) (2015) 41494.
[155] R.S. Chen, S. Ahmad, S. Gan, Rice husk bio-filler reinforced polymer blends of recycled HDPE/PET: three-dimensional stability under water immersion and mechanical performance, Polym, Compos 39 (8) (2018) 2695–2704.
[156] A. Marotta, A. Causa, M. Salzano de Luna, V. Ambrogi, G. Filippone, Tuning the morphology of HDPE/PP/PET ternary blends by nanoparticles: a simple way to improve the performance of mixed recycled plastics, Polymers 14 (24) (2022) 5390.
[157] M.C. Mistretta, M. Morreale, F.P. La Mantia, Thermomechanical degradation of polyethylene/polyamide 6 blend-clay nanocomposites, Polym. Degrad. Stabil. 99 (2014) 61–67.